Characterization of Shear Stratified Turbulence Around a Jet Stream: Mesoscale-Microscale Approach

and

Variability and Statistics of Shear Stratified Turbulence Outer Scales Around a Jet Stream

Alex Mahalov and Basil Nichols
Program in Environmental Fluid Dynamics
Arizona State University

ASU Team

H. J. S. Fernando, B. Joseph,
A. Mahalov, B. Nichols, K. L. Tse

Issues of Atmospheric Turbulence for ABL/ADA (Atmospheric Decision Aid)

- ABL beam propagates (at small horizontal angles) through a turbulent field neither homogeneous, nor isotropic.
- Turbulence around atmospheric tropopause has length scales with strong vertical variability.
- Turbulence phenomenology characterized by intermittent layers of weak and strong refractive index (C_n^2)variability.
- Non-Kolmogorov turbulence effects over long propagation paths.
- For subtropical and/or polar jet streams, we evidence two such layers on edges of jet stream.

- Correlation with mesoscale atmospheric dynamics (WRF, MM5 codes), data from the latter to be inputted on a coarse grid.
- Our goal: parametrization of vertical C_n^2 profiles (averaged over horizontal scales of ABL beam propagation).

Payoff:

- Parametrization and vertical variability of turbulence outer length scales, temperature fluctuations and related physical quantities required for propagation codes; "catalogue" for a representative set of atmospheric events around the tropopause, of relevance to ABL/ADA.
- System performance modeling and determination of performance bounds via simulation of both average atmospheric events and more extreme atmospheric events of relevance to ABL/ADA.

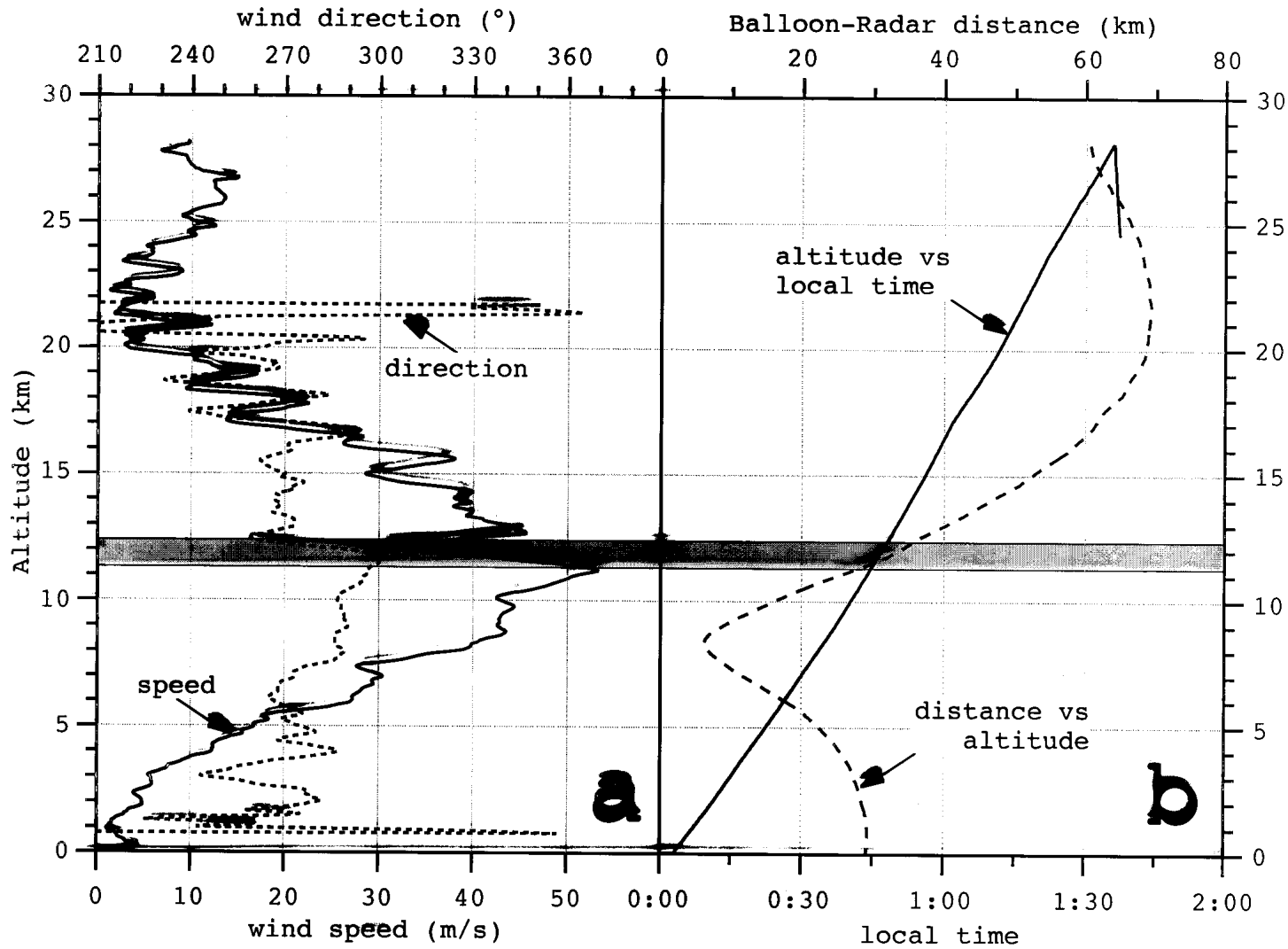

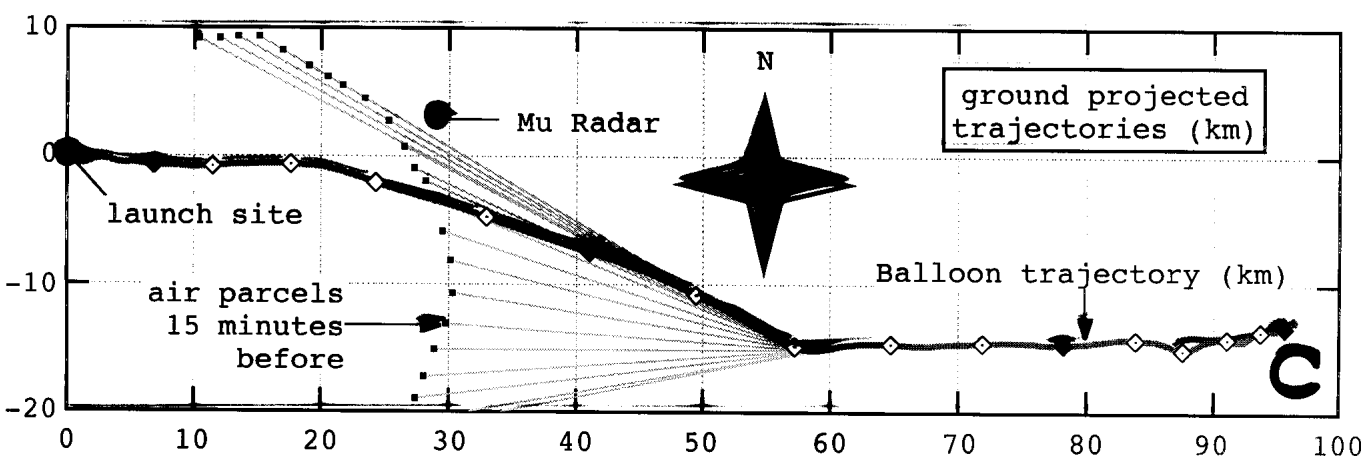

(Sea of Japan)

COURTESY
F. Dalaudier

(vertical)

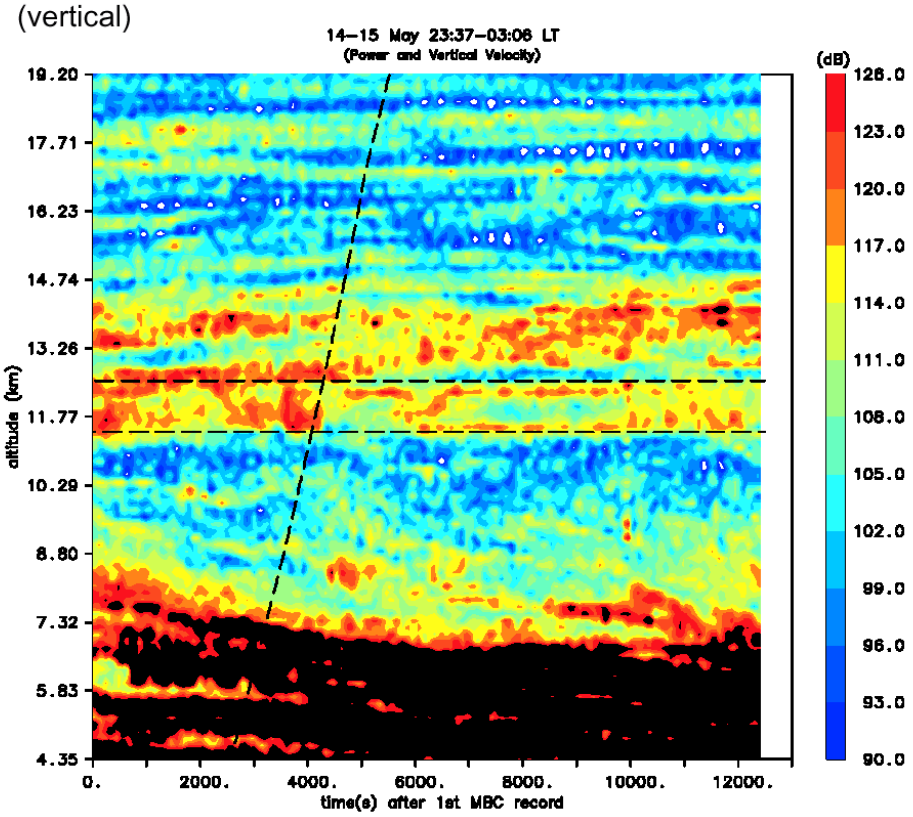

(oblique, 12 deg. off zenith)

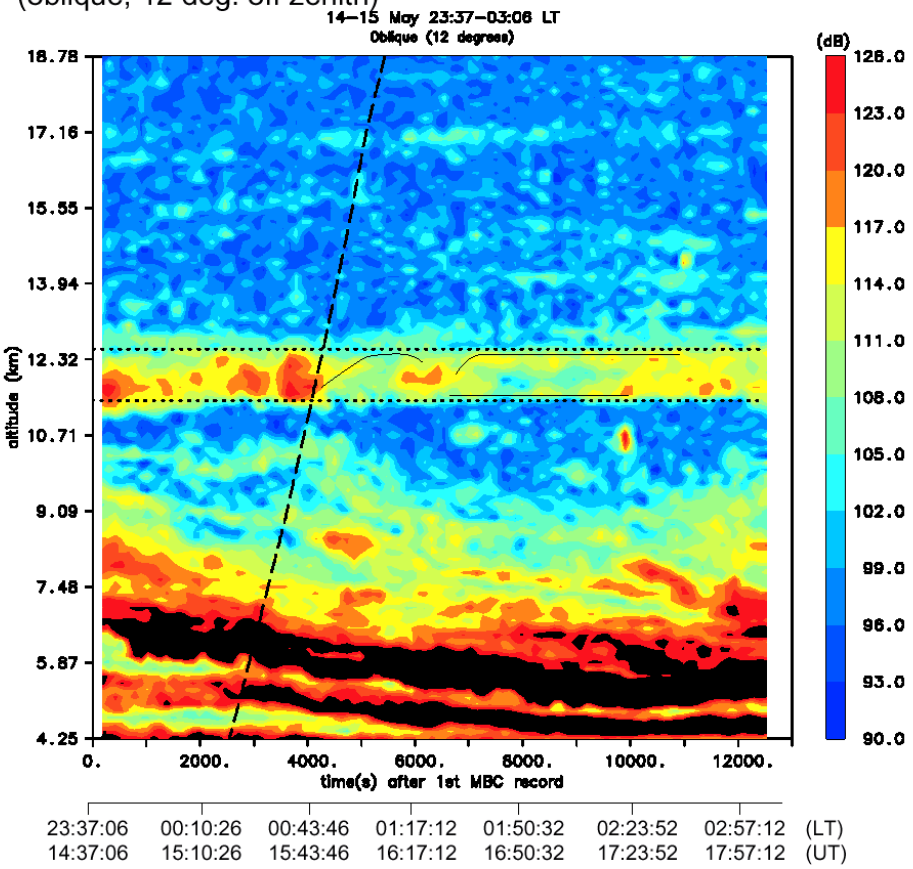

"THIN LAYERS

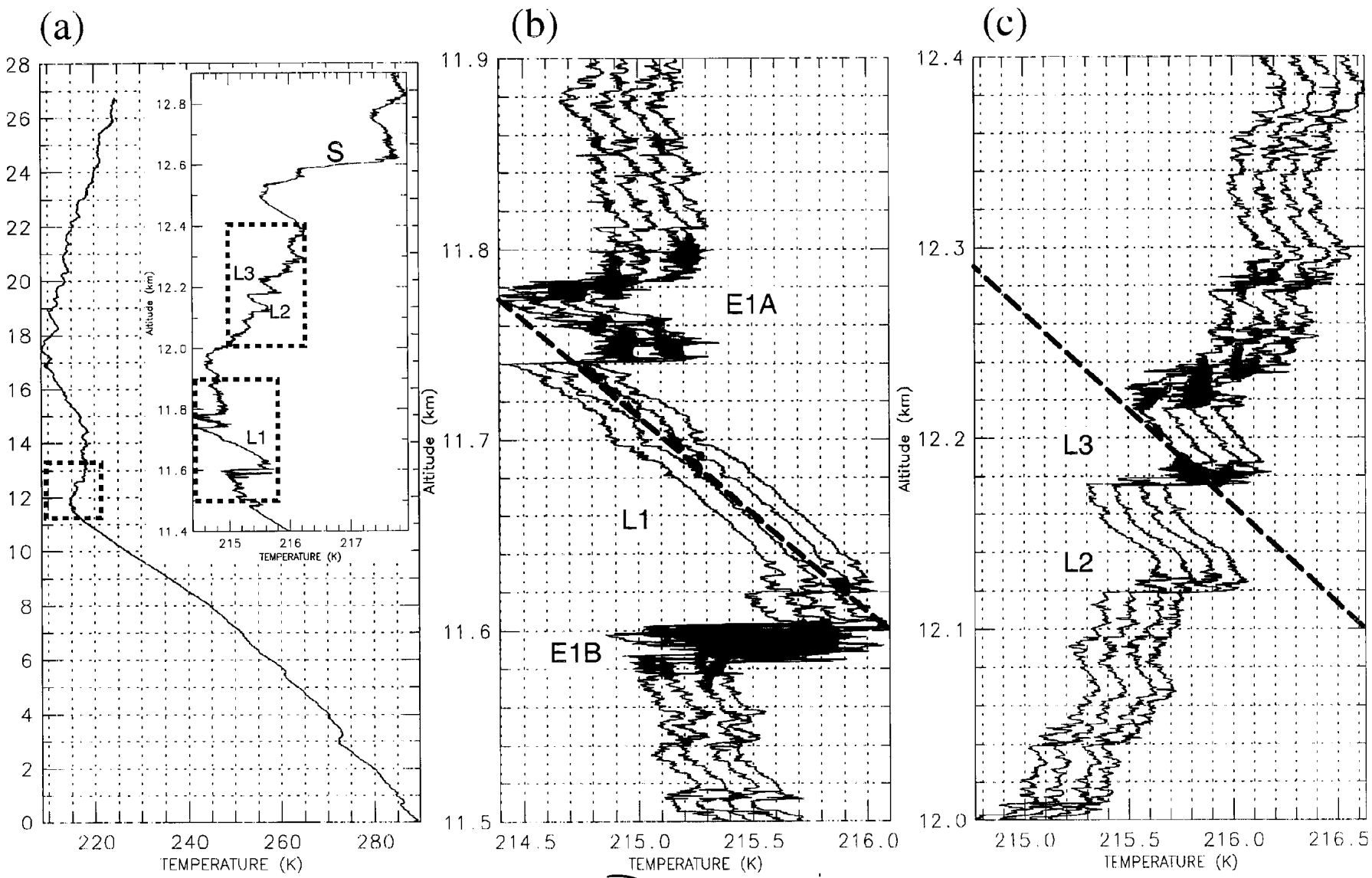

F. DALAUDIER

Sea OF JAPAN

"THIN LAYERS"

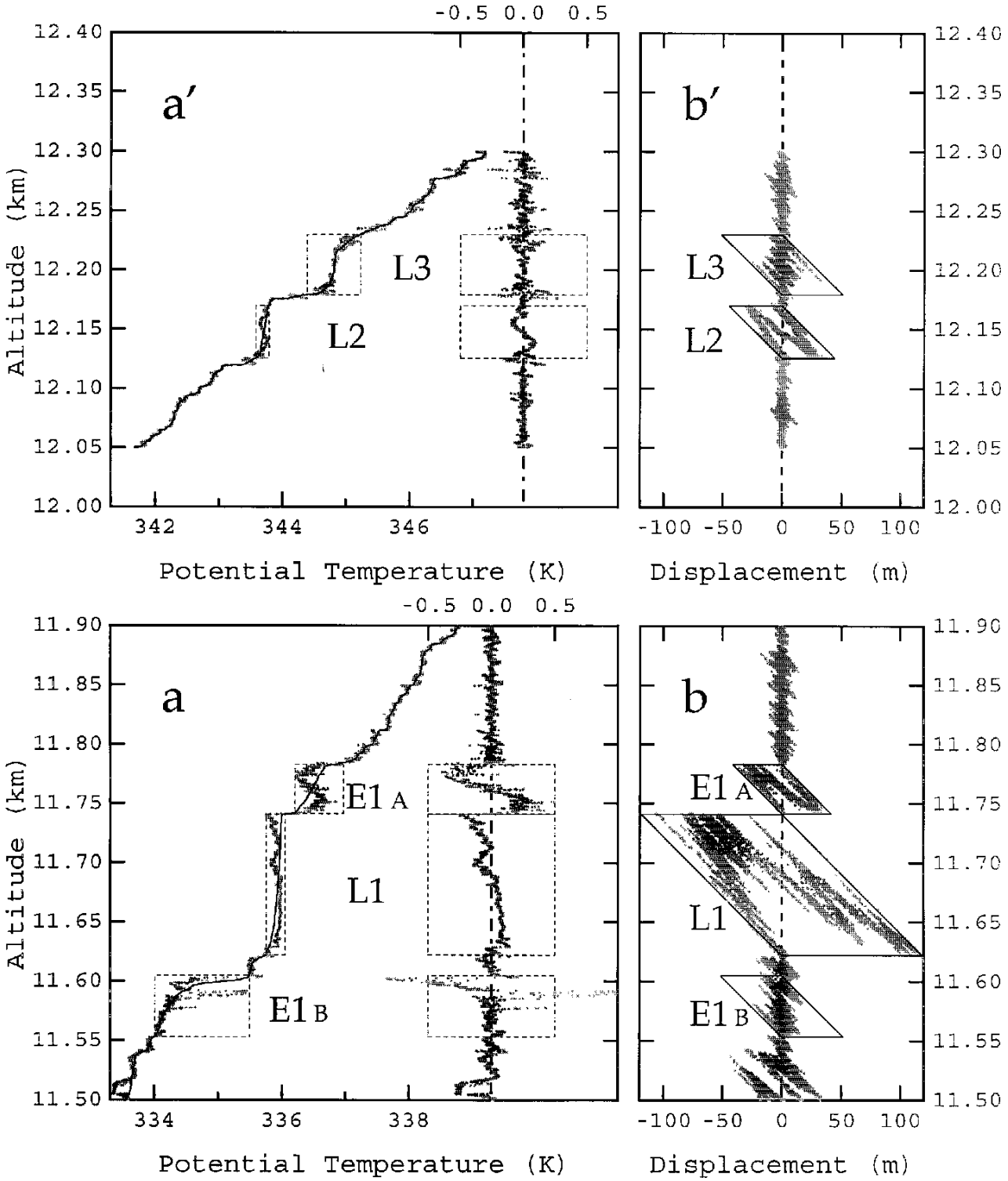
a′
b′
L3
L2
a
b
E1 A
L1
E1 B
Altitude (km)
Potential Temperature (K)
Displacement (m)
-0.5 0.0 0.5
12.40
12.35
12.30
12.25
12.20
12.15
12.10
12.05
12.00
342
344
346
-100 -50 0 50 100
11.90
11.85
11.80
11.75
11.70
11.65
11.60
11.55
11.50
334
336
338

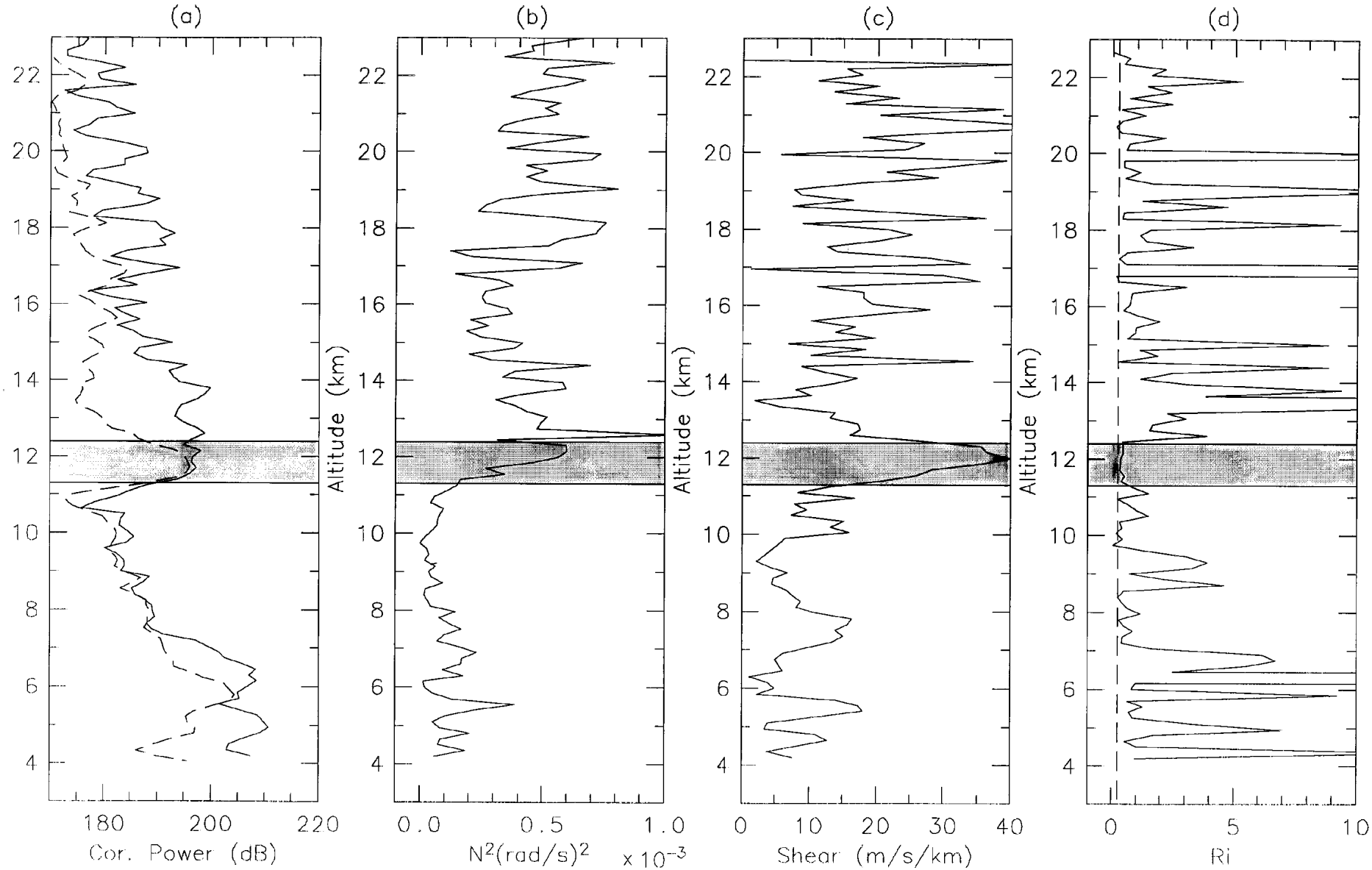
(a)
(b)
(c)
(d)
Altitude (km)
Cor. Power (dB)
N²(rad/s)² x 10⁻³
Shear (m/s/km)
Ri

Outline of Synoptic Situation and Turbulence Calculation.

Case based on jet profile by Bedard, Canavero and Einaudi (1986) *J. Atmos. Sci.* **43**, 2838-2844.

20 February 1973

Sounding data from NCAR lee wave program and accompanying turbulence reports from aircraft.

MM5 V3 Initialized with NCEP Reanalysis.

Run on 90km-30km nested grid with 62 vertical levels to generate dynamically consistent mass and momentum fields.

Model jet and thermal field agree with that in Bedard et.al.

Developing jet (MM5 simulation)

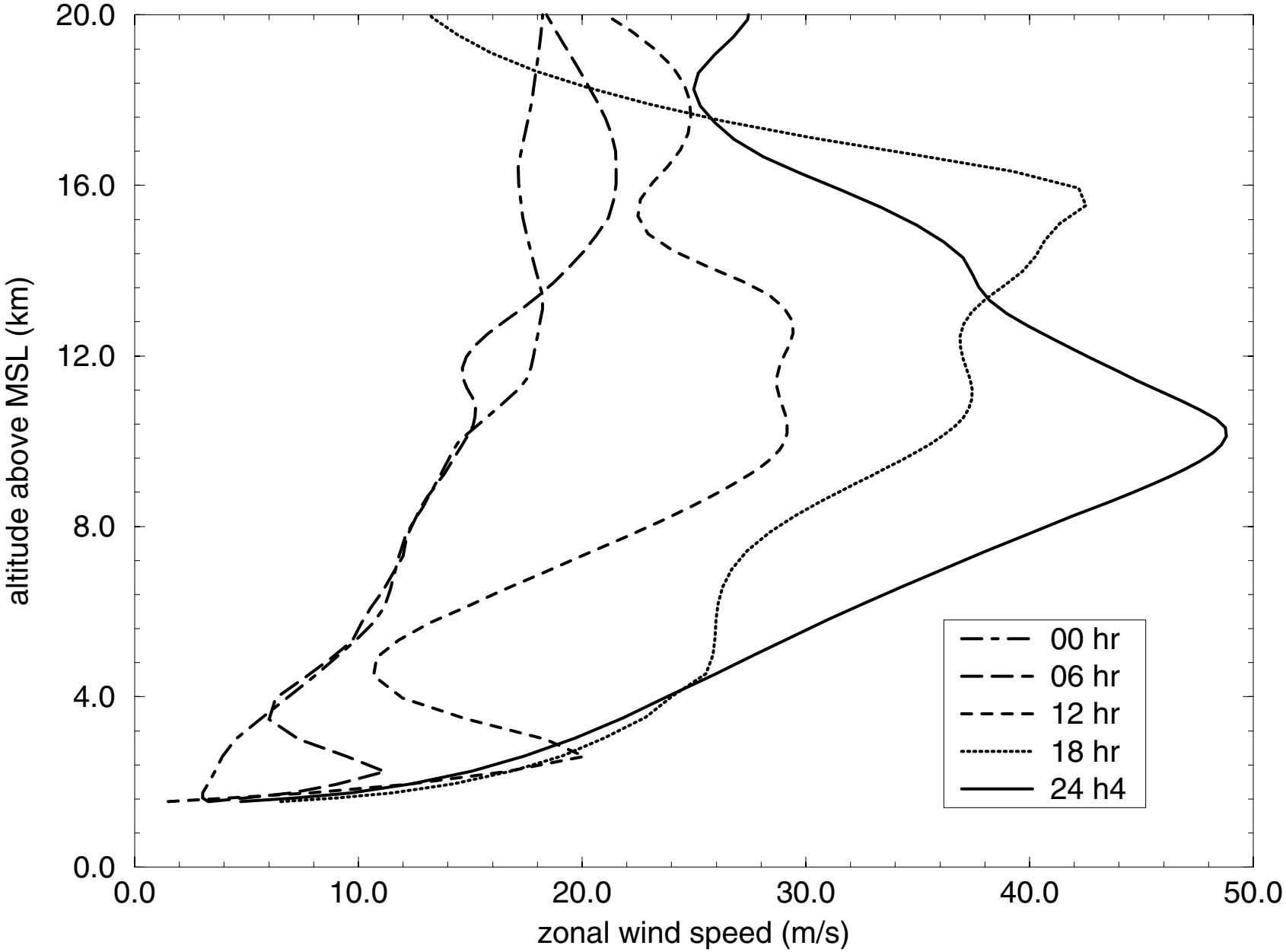

JET 2030 UT, 20 Feb 1973

Continental Divide (40.1 N, 105.7 W)

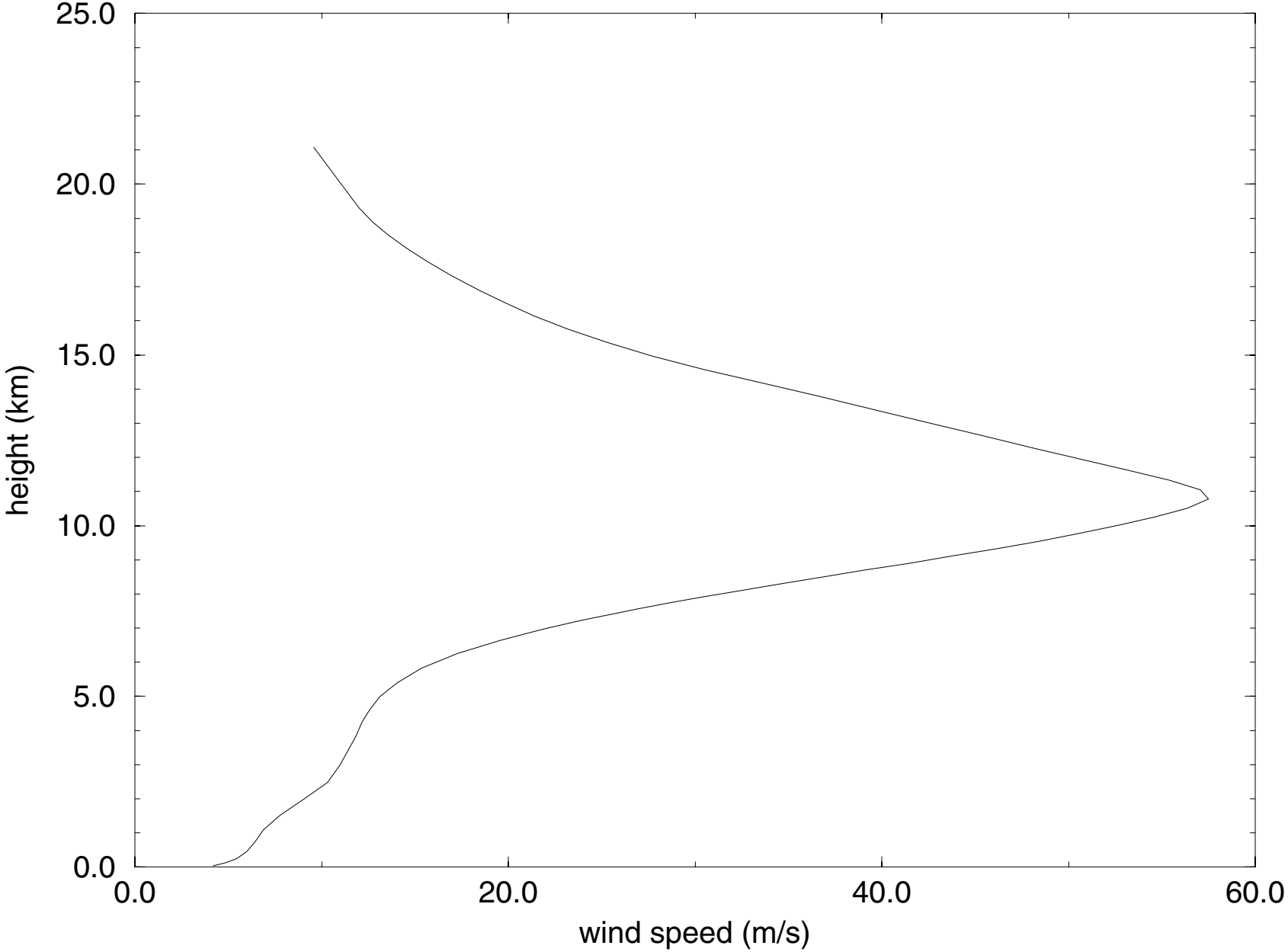

Microscale Meteorological Modeling of C_n^2 for ABL Propagation Codes

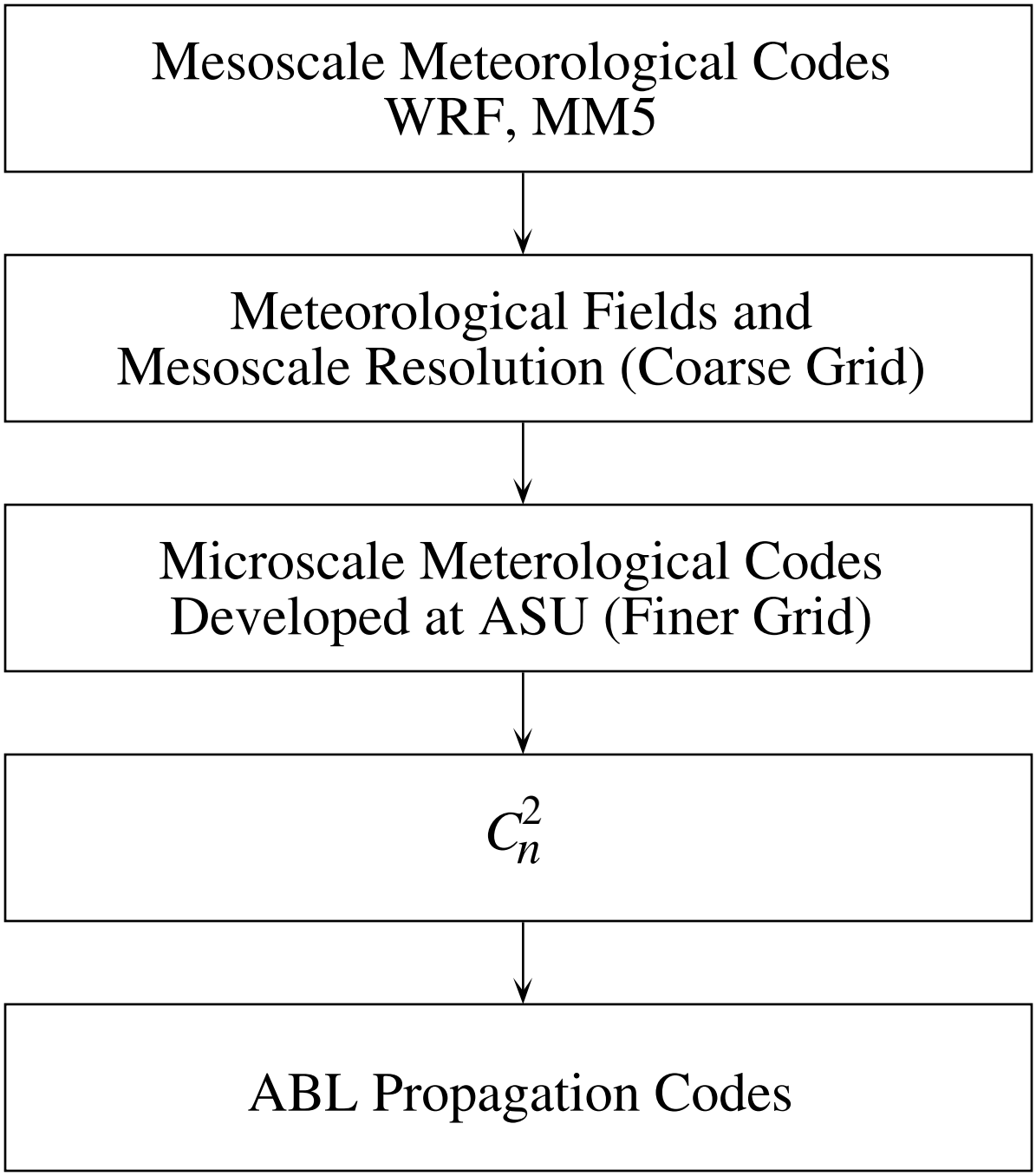

MM5 is used to predict meteorological fields on a coarse grid (mesoscale). This information is used as an input to microscale DNS codes which resolve scales relevant for ABL propagation codes.

Numerical methods
Spectral Domain Decomposition

- Spectral method are used for spatial derivatives. The variables are transformed to Fourier space in horizontal directions. In the vertical direction, the computational domain is divided into subdomains and a mixture of collocation and variational methods are used for the subdomains.
- Time splitting scheme: the nonlinear and body force terms are advanced in the first substep, pressure adjustment in the second substep and viscous terms in the third substep.
- The program is parallelized by method of transposition and mpi is used for message passing.
- The simulation is carried out on the massively parallel Bluemountain machine at Los Alamos National Laboratory and ARL MSRC.

In the vertical direction spectral domain decomposition method is employed.

- The domain is divided into subdomains (in the vertical direction) and each subdomain is mapped individually to [-1,1]
- In each subdomain the variables are interpolated with Lagrangian interpolation using Legendre-Gauss-Lobatto points.
- Collocation method is used to calculate spatial derivatives in the vertical direction.

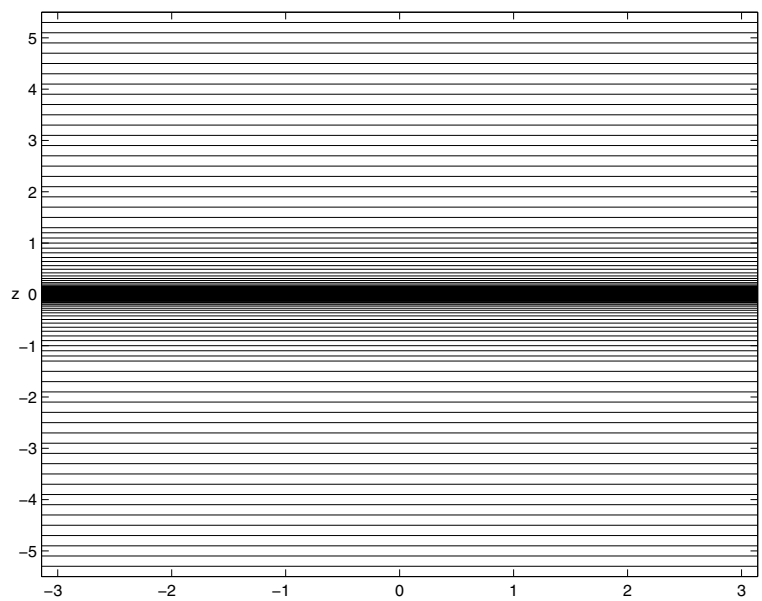

Subdomain Boundaries

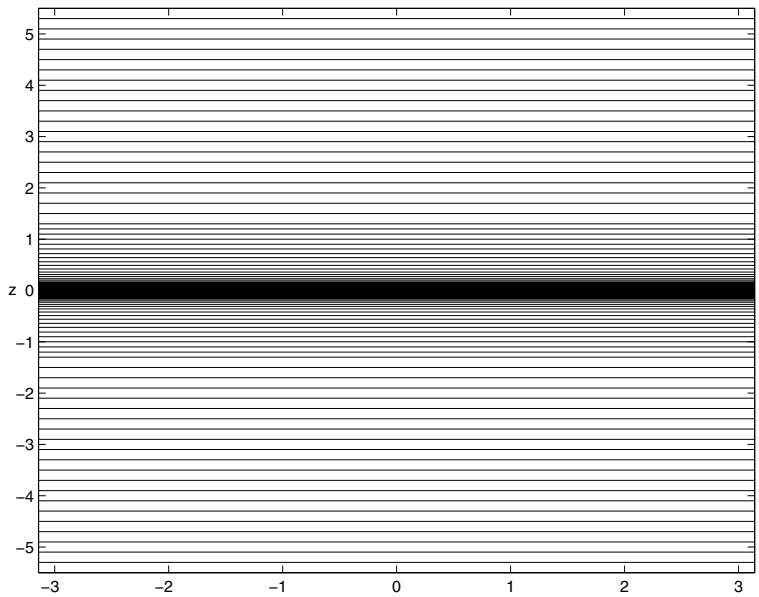

- resolution in vertical : 1024
- # of subdomain : 255

Bedard, Canavero & Einaudi, JAS, **43**, 23, (1986)

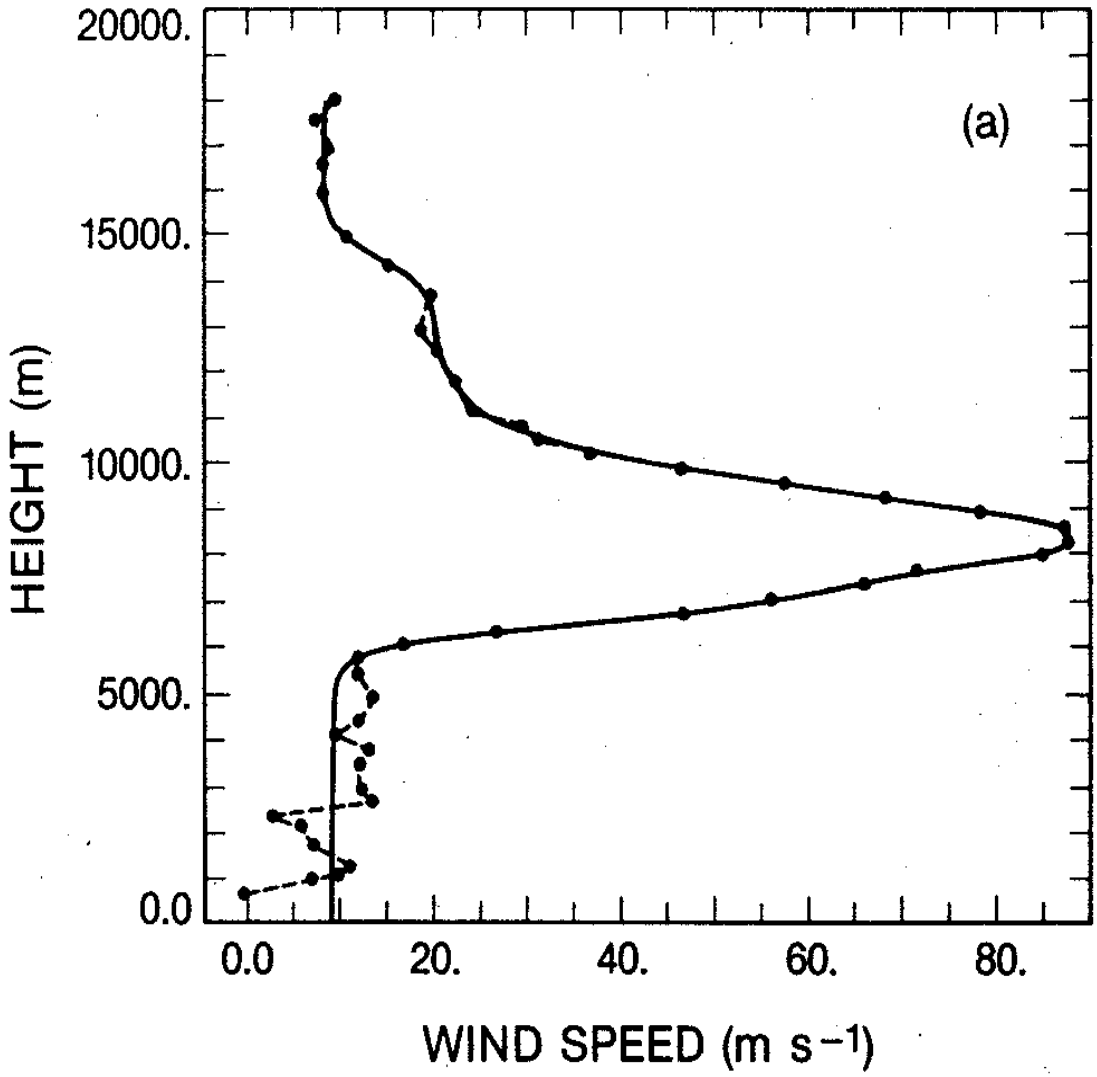

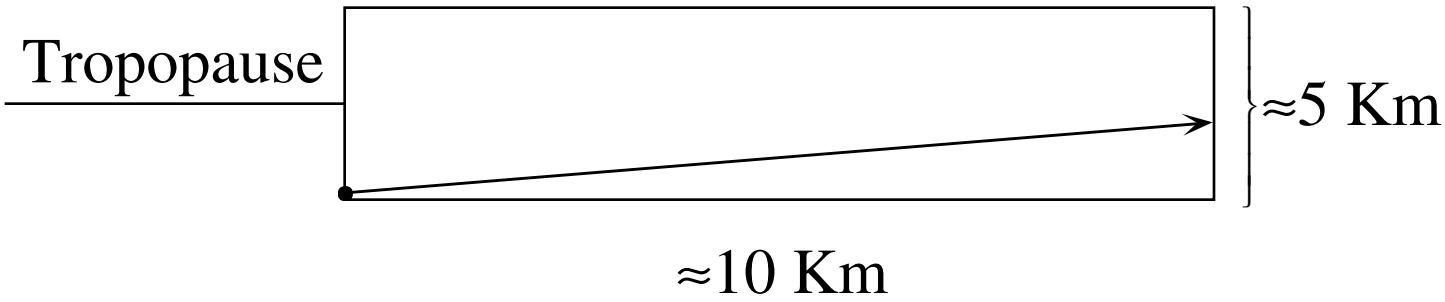

Computational Domain for
Microscale Meteorological Codes

- Strong nonlinear interaction between potential vorticity dynamics and inertio-gravity waves, topography gravity waves, gravity currents, jet streaks

- Microscale nonlinear dynamics of thermal wind imbalance and divergent velocity potential

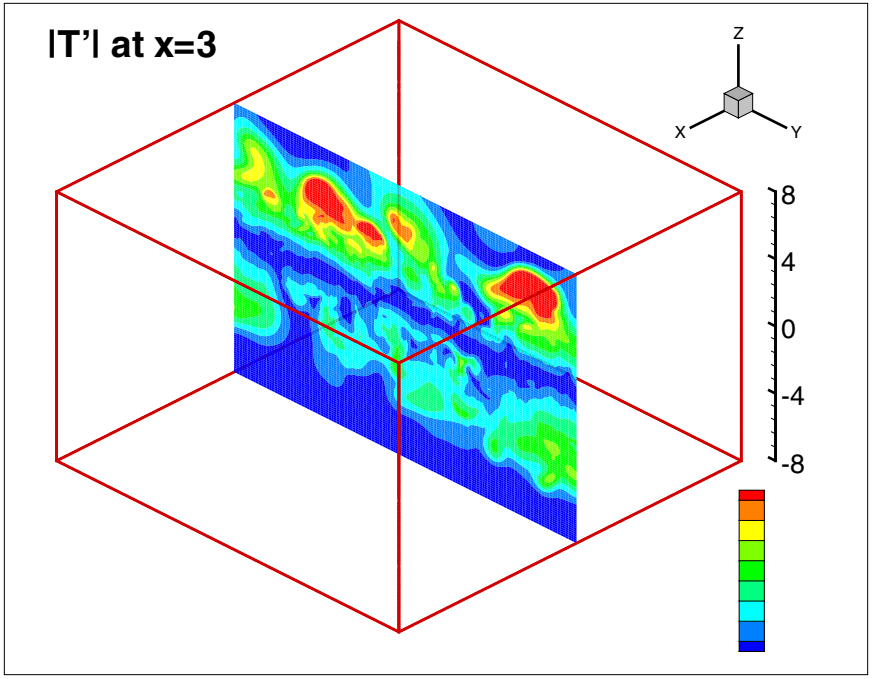
|T'| at x=3
Z
X
Y
8
4
0
-4
-8

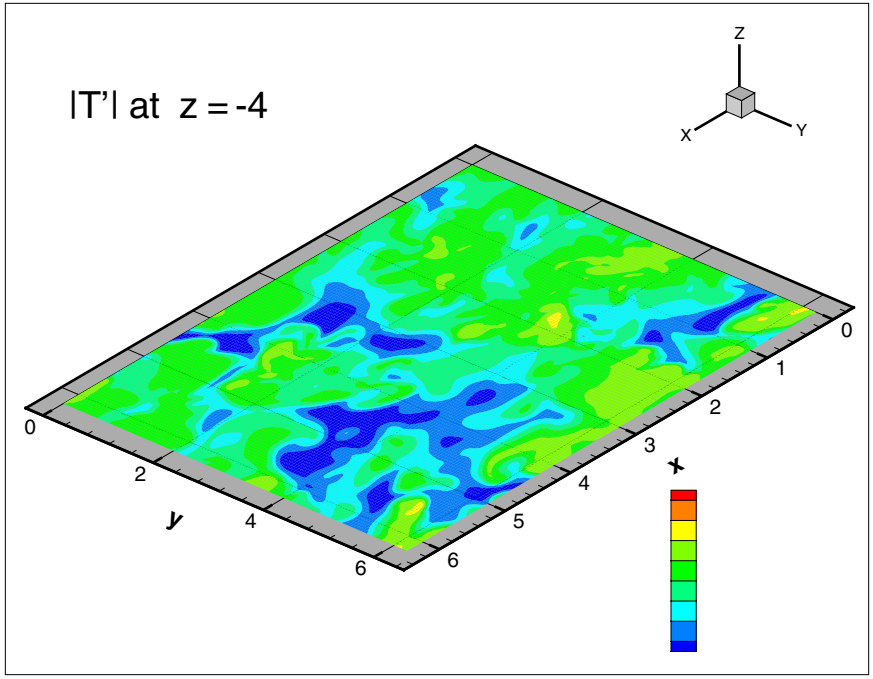
|T'| at z = -4
Z
X
Y
0
2
4
6
y
0
1
2
3
4
5
6
x

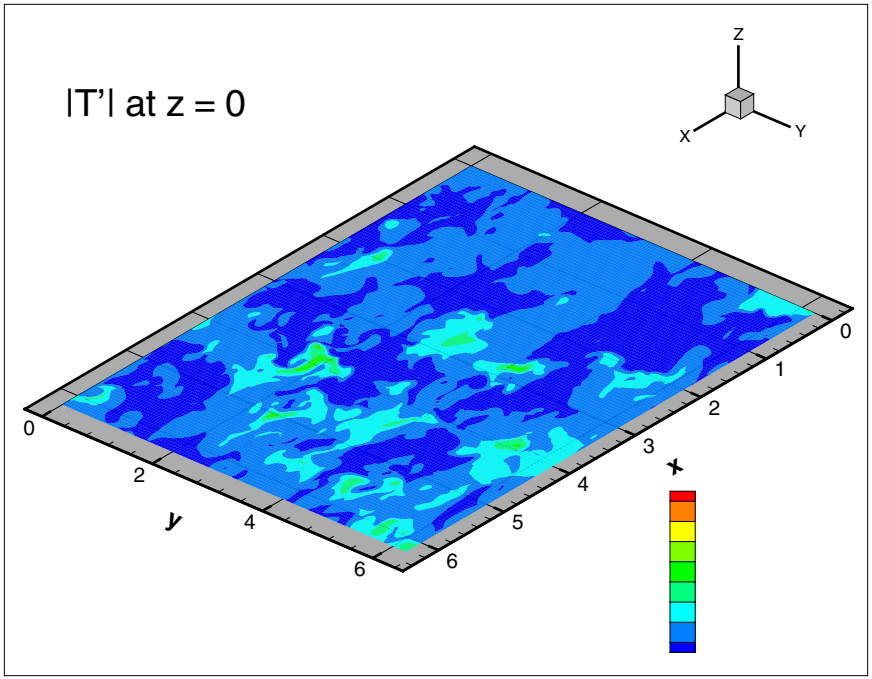
|T'| at z = 0
Z
X
Y
0
2
4
6
y
0
1
2
3
4
5
6
x

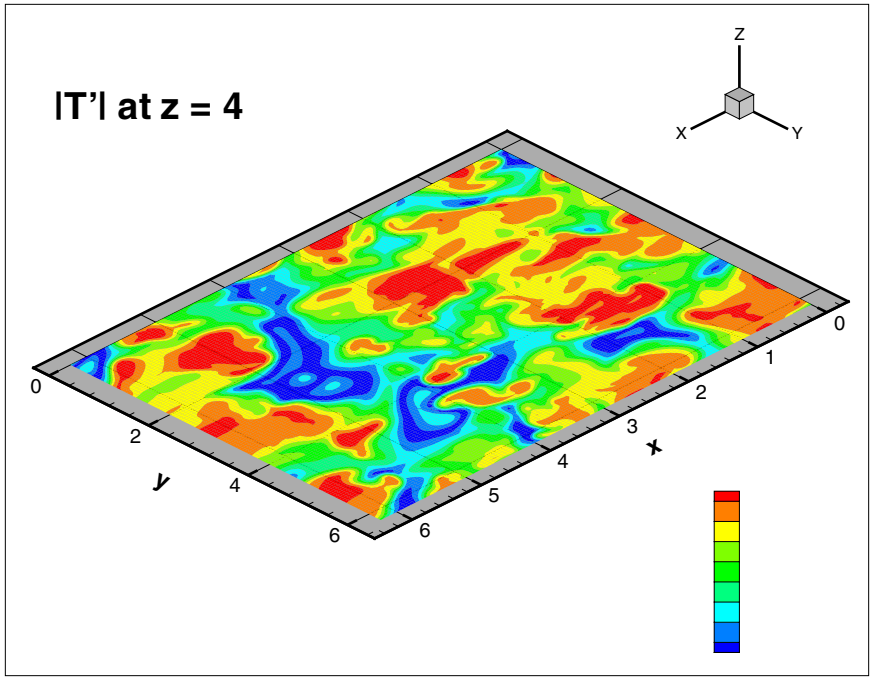
|T'| at z = 4
Z
X
Y
0
2
4
6
y
0
1
2
3
4
5
6
x

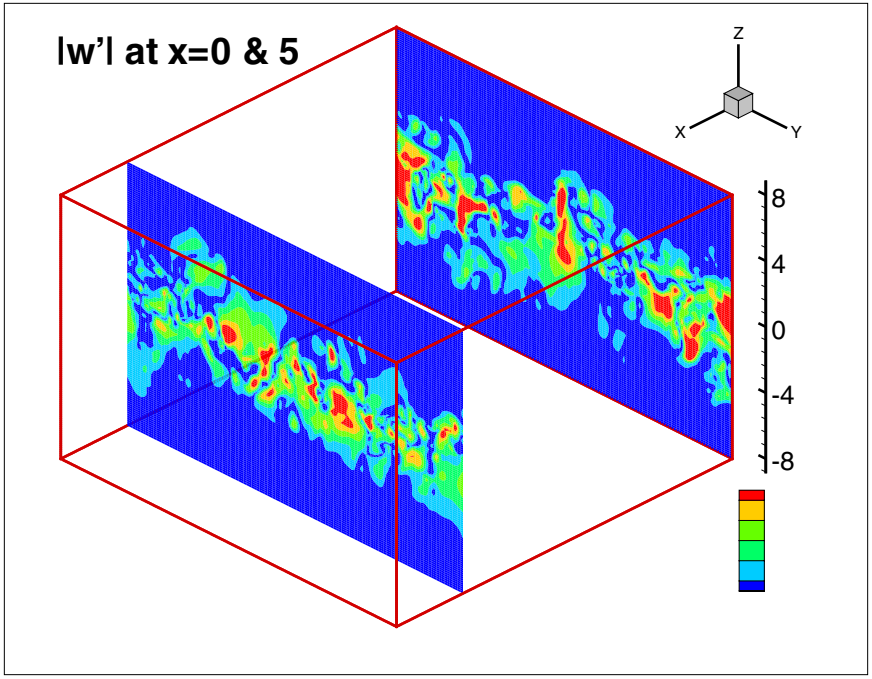
|w'| at x=0 & 5
Z
X
Y
8
4
0
-4
-8

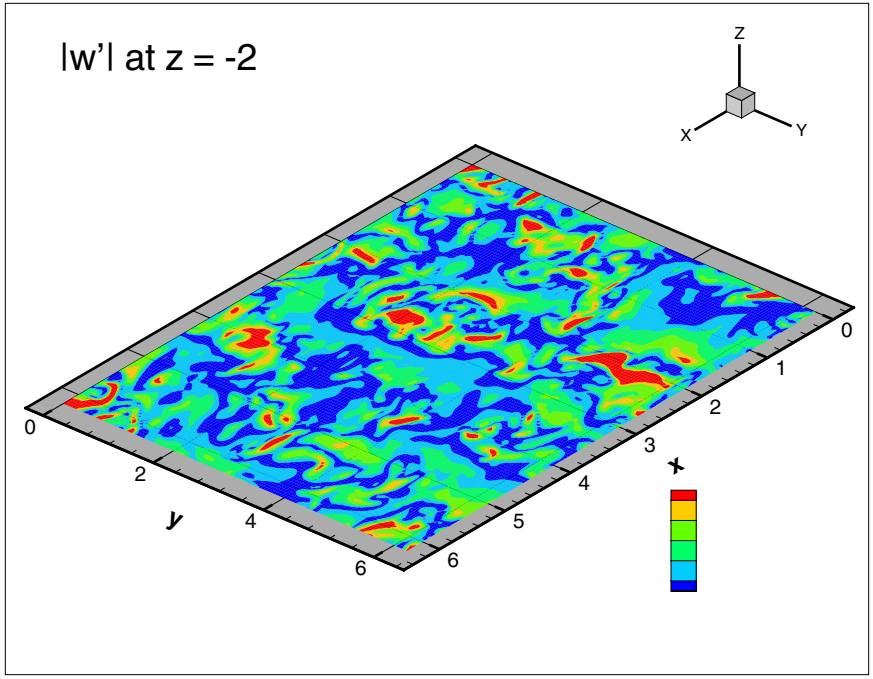
|w'| at z = -2
Z
X
Y
0
2
4
6
y
0
1
2
3
4
5
6
x

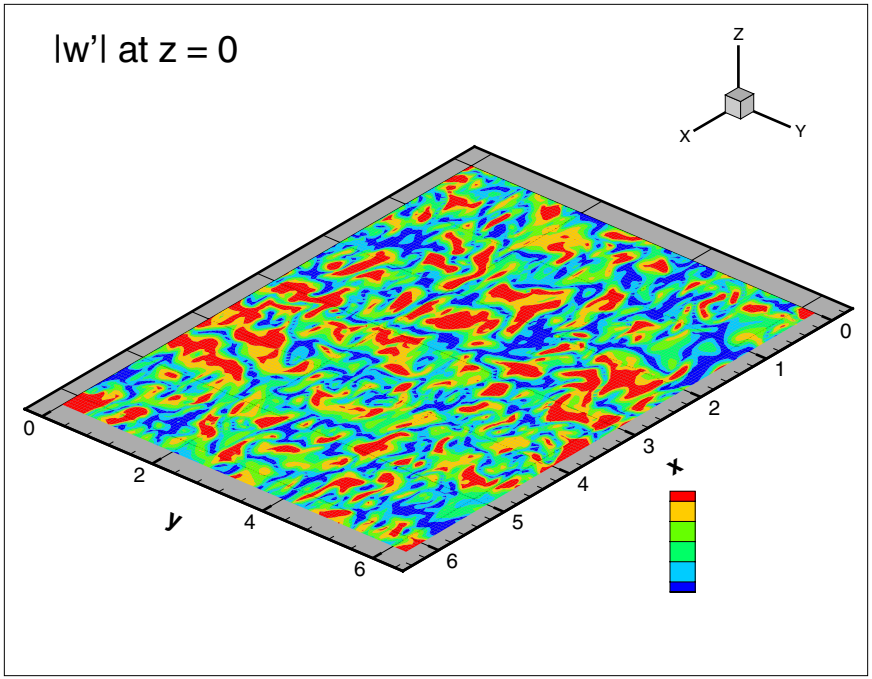
|w'| at z = 0
Z
X
Y
0
2
4
6
y
0
1
2
3
4
5
6
x

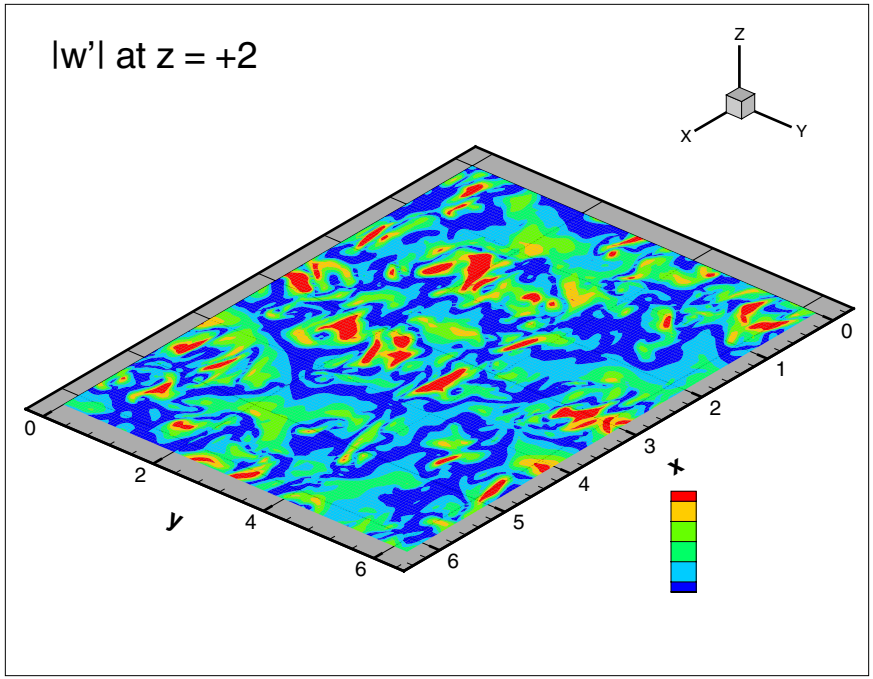
|w'| at z = +2
Z
X
Y
0
2
4
6
y
0
1
2
3
4
5
6
x

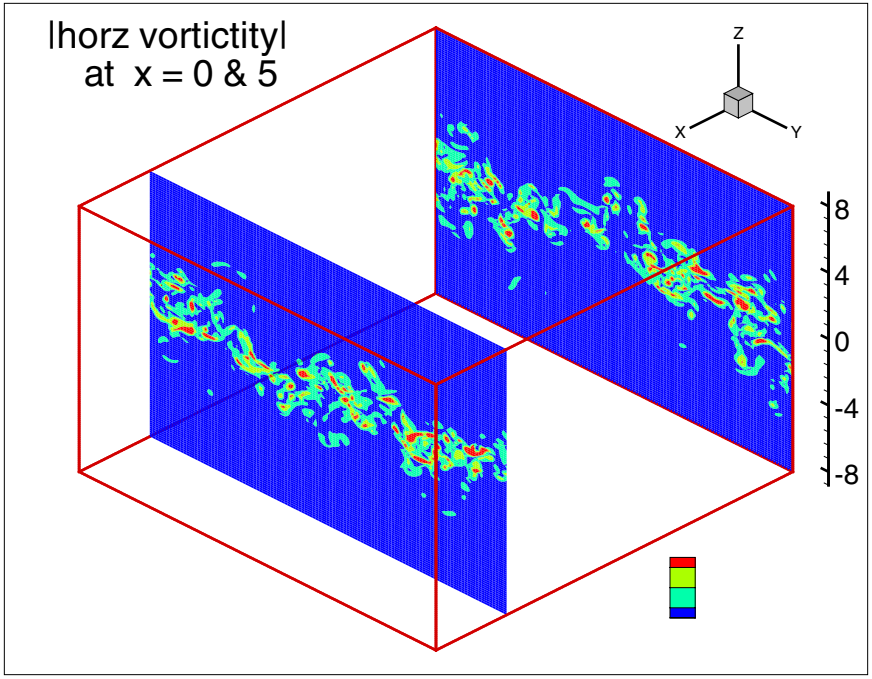
|horz vortictity|
at x = 0 & 5
Z
X
Y
8
4
0
-4
-8

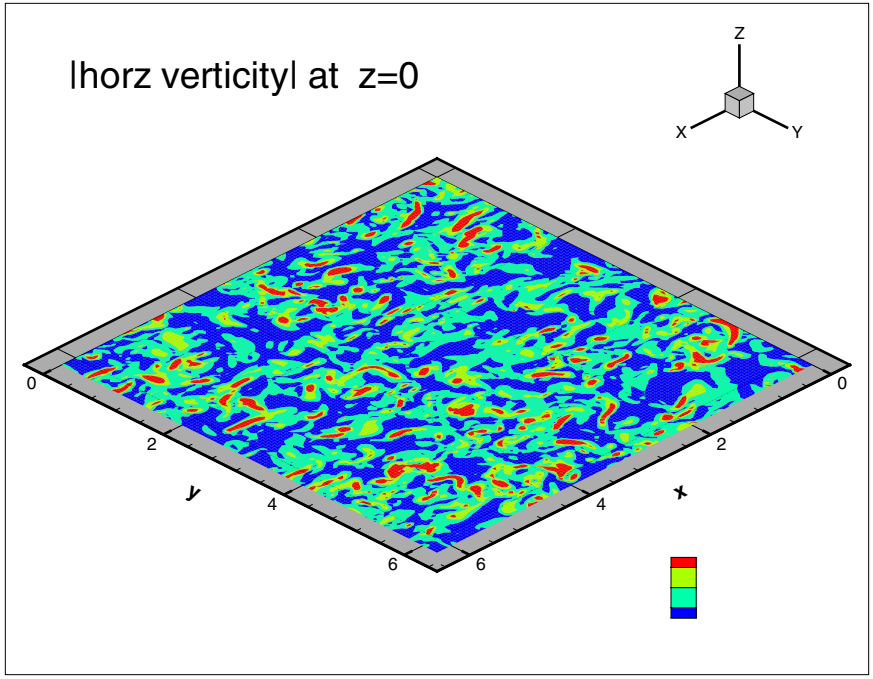
|horz verticity| at z=0
Z
X
Y
0
2
4
6
y
0
2
4
6
x

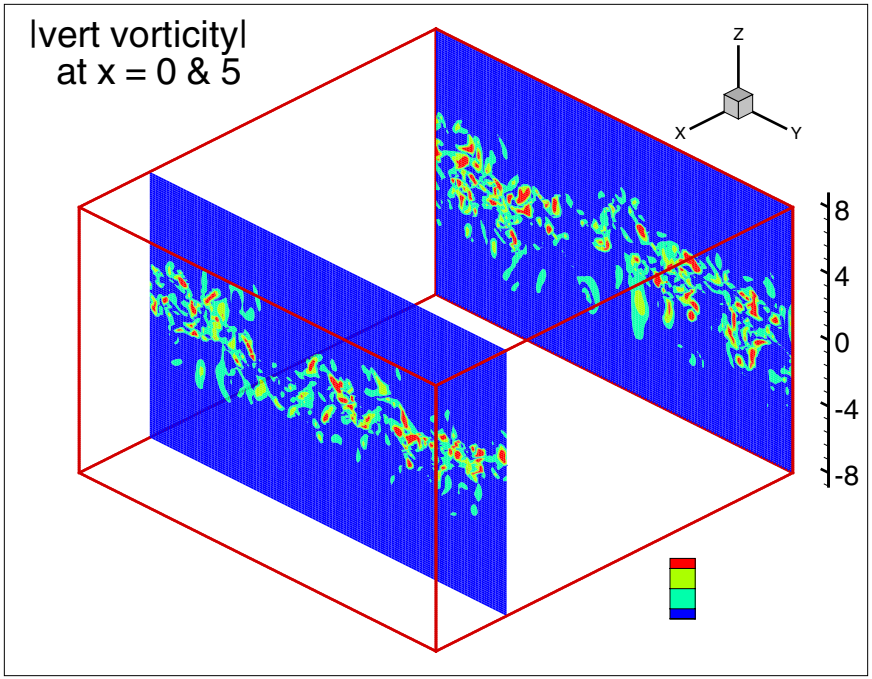
|vert vorticity|
at x = 0 & 5
Z
X
Y
8
4
0
-4
-8

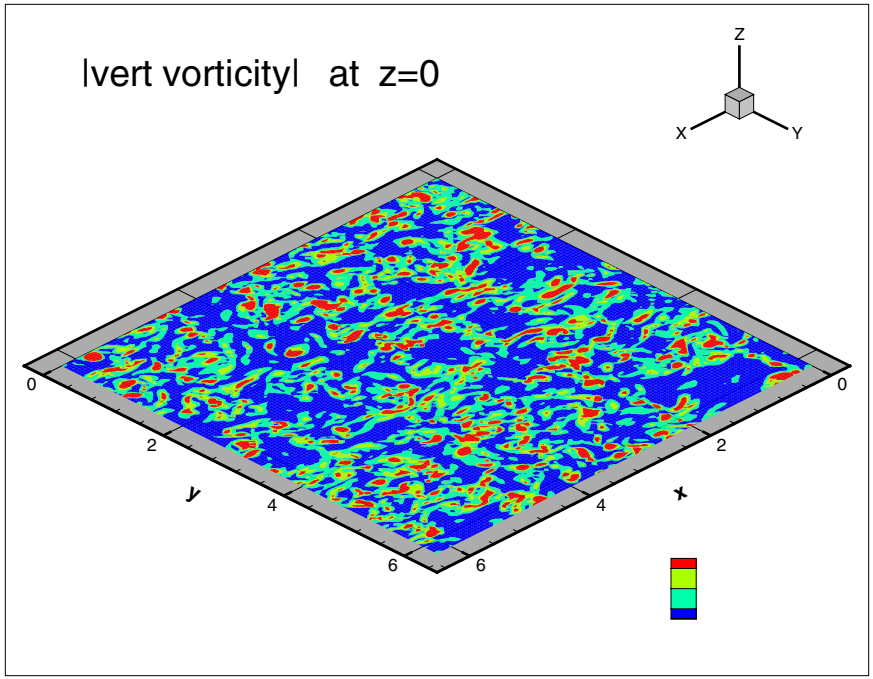
|vert vorticity| at z=0
Z
X
Y
0
2
4
6
y
0
2
4
6
x

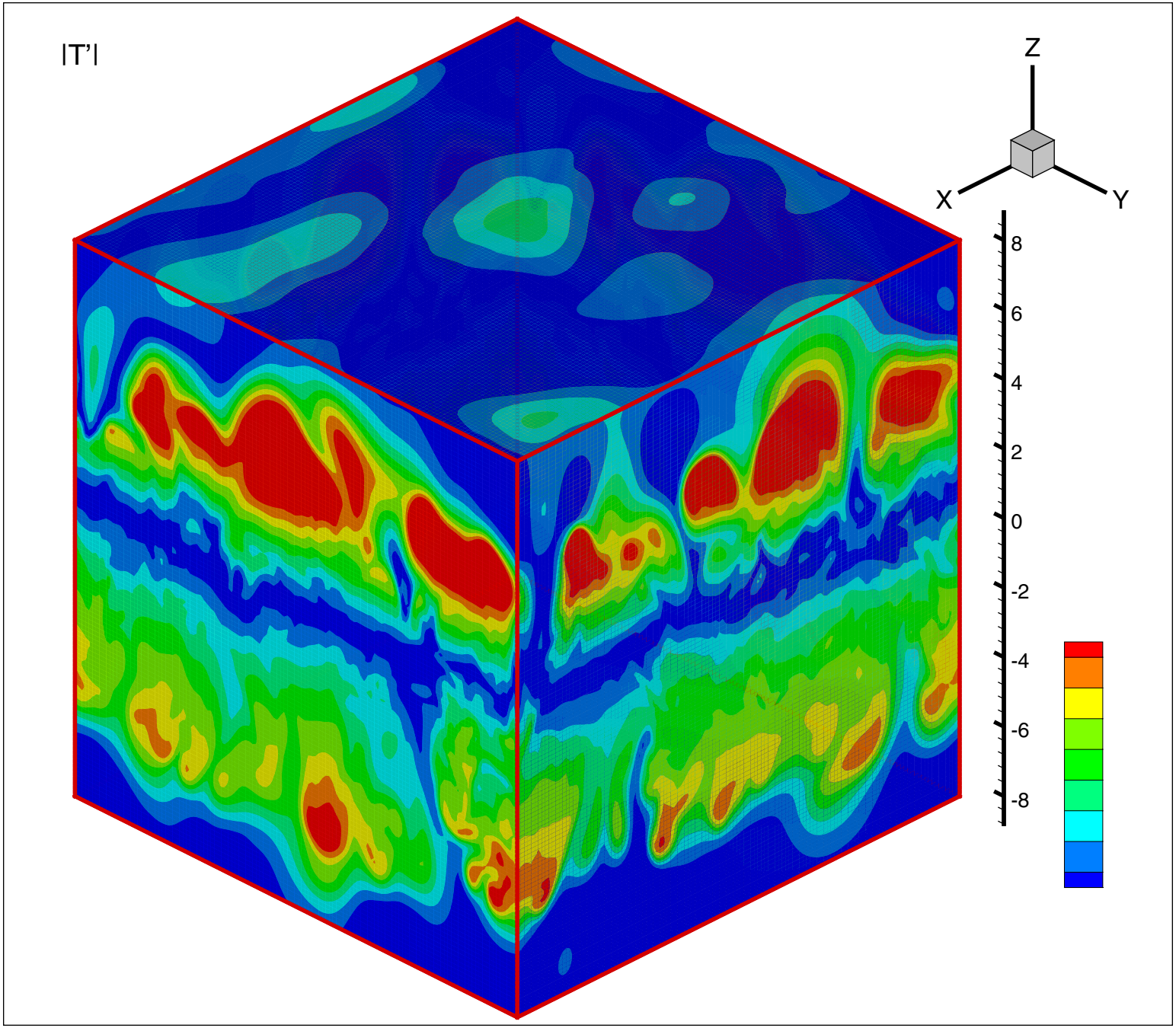
|T'|
Z
X
Y
8
6
4
2
0
-2
-4
-6
-8

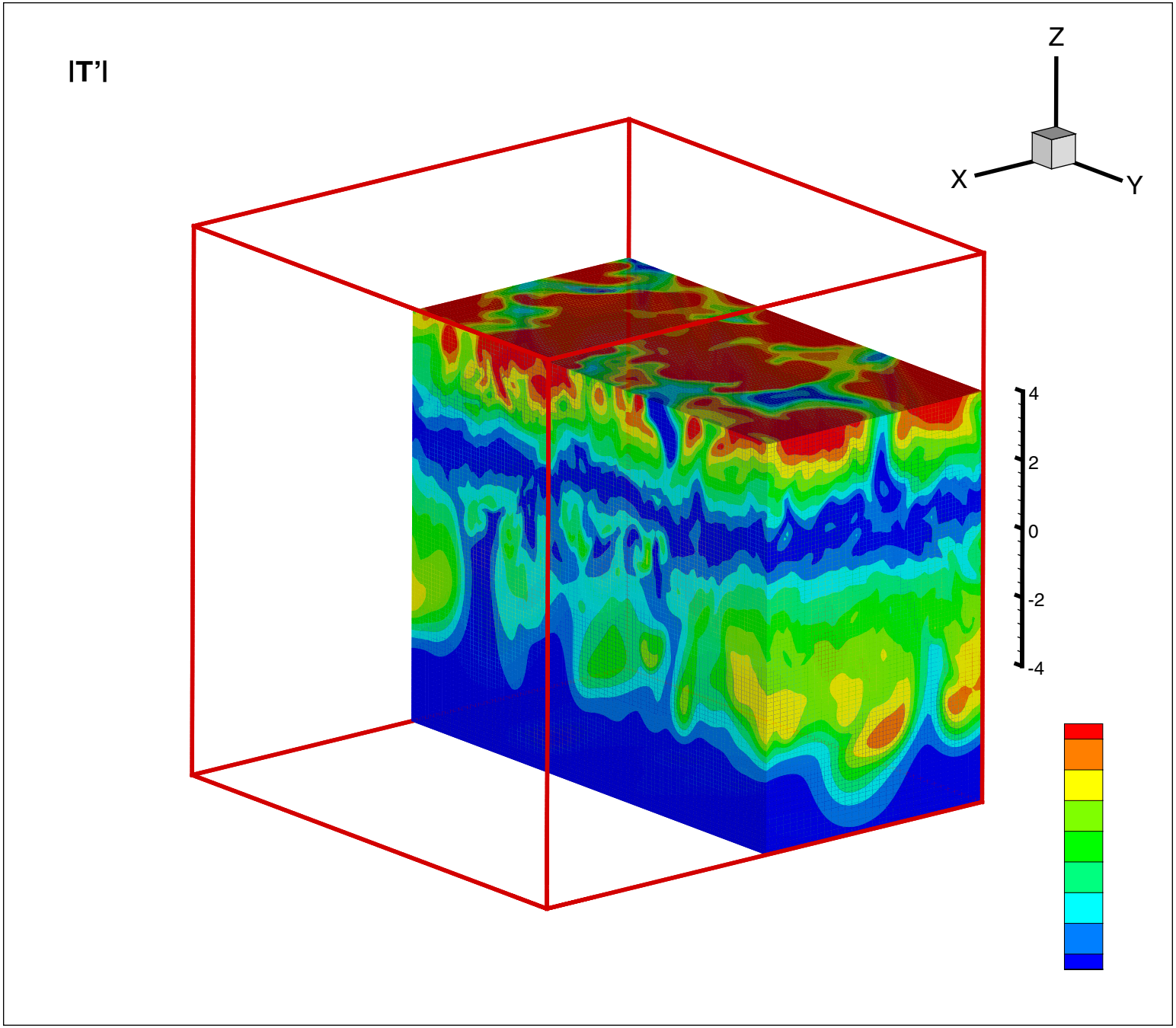
IT'I
Z
X
Y
4
2
0
-2
-4

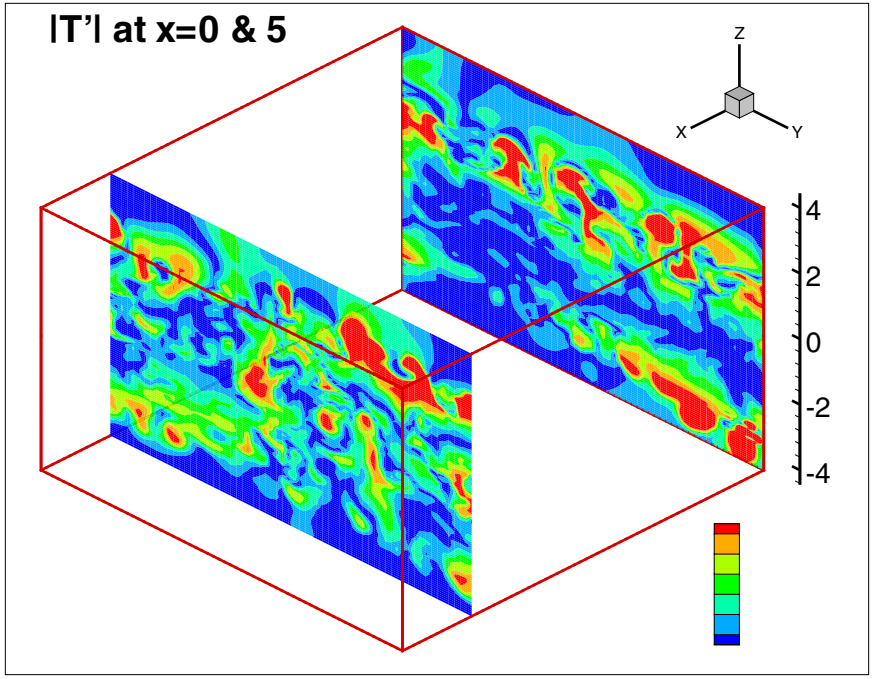
|T'| at x=0 & 5
Z
X
Y
4
2
0
-2
-4

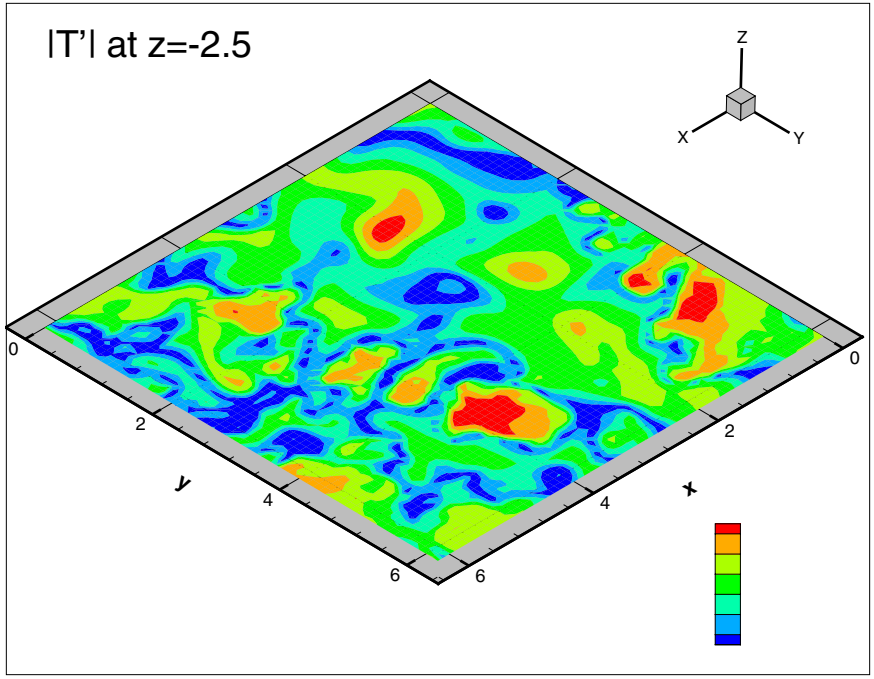
|T'| at z=-2.5
Z
X
Y
0
2
4
6
y
0
2
4
6
x

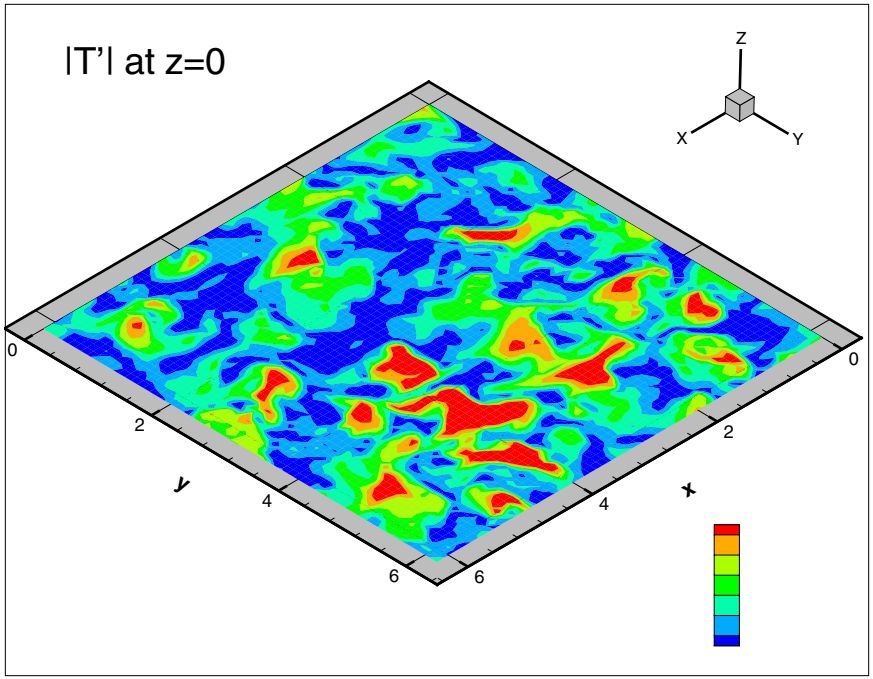
|T'| at z=0
Z
X
Y
0
2
4
6
y
0
2
4
6
x

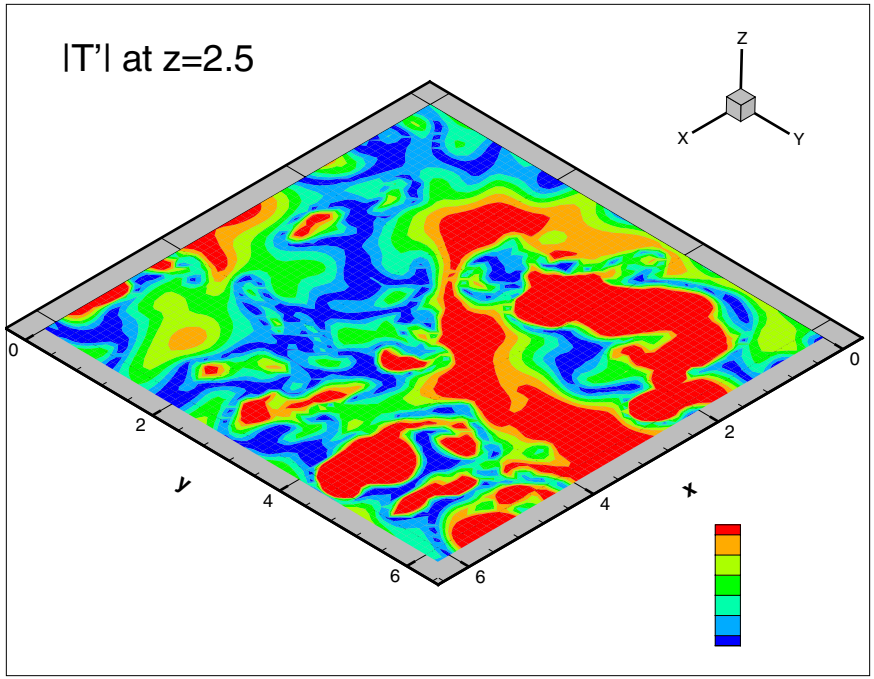
|T'| at z=2.5
Z
X
Y
0
2
4
6
y
0
2
4
6
x

Wavelet Analysis

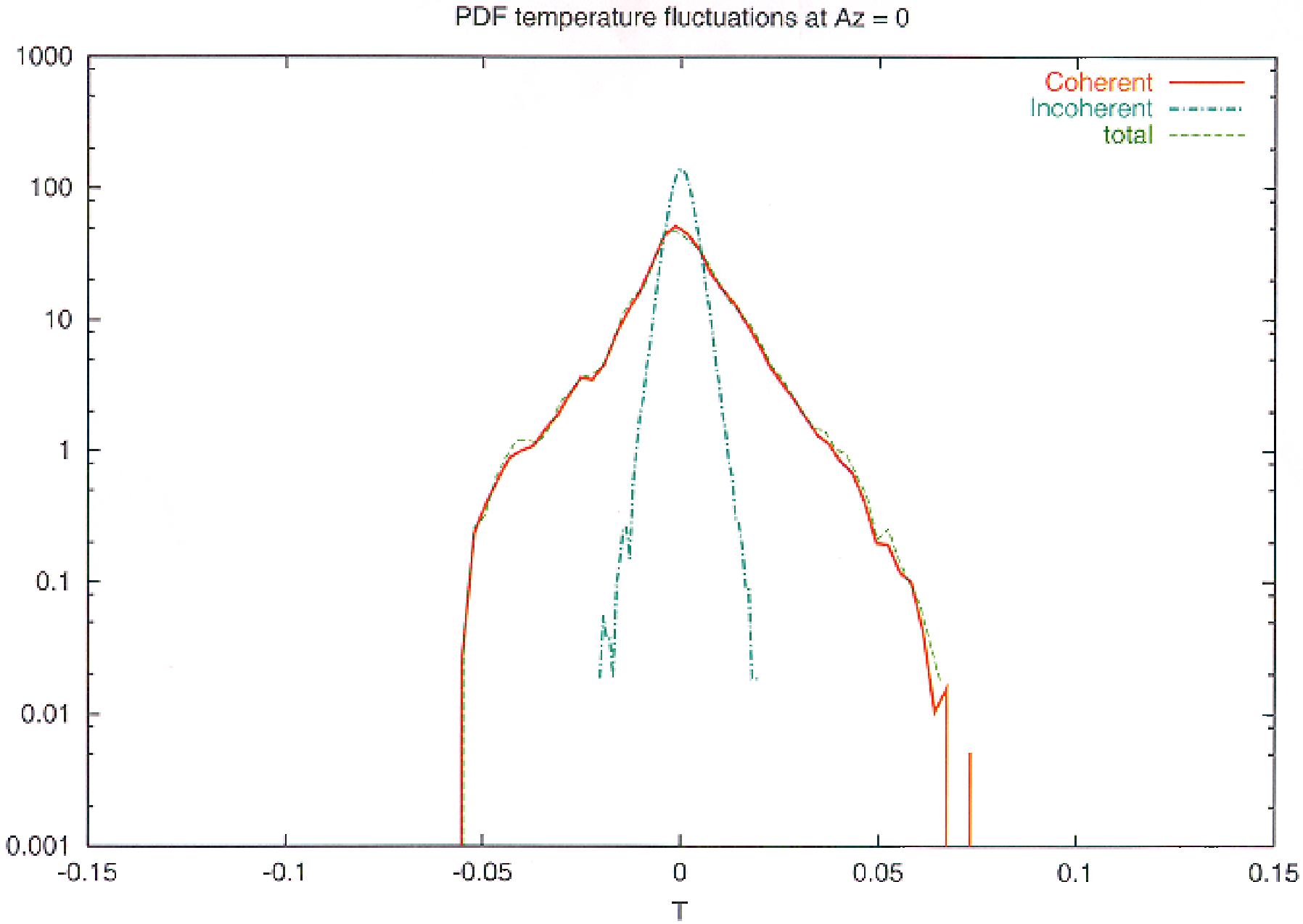

Wavelet Analysis

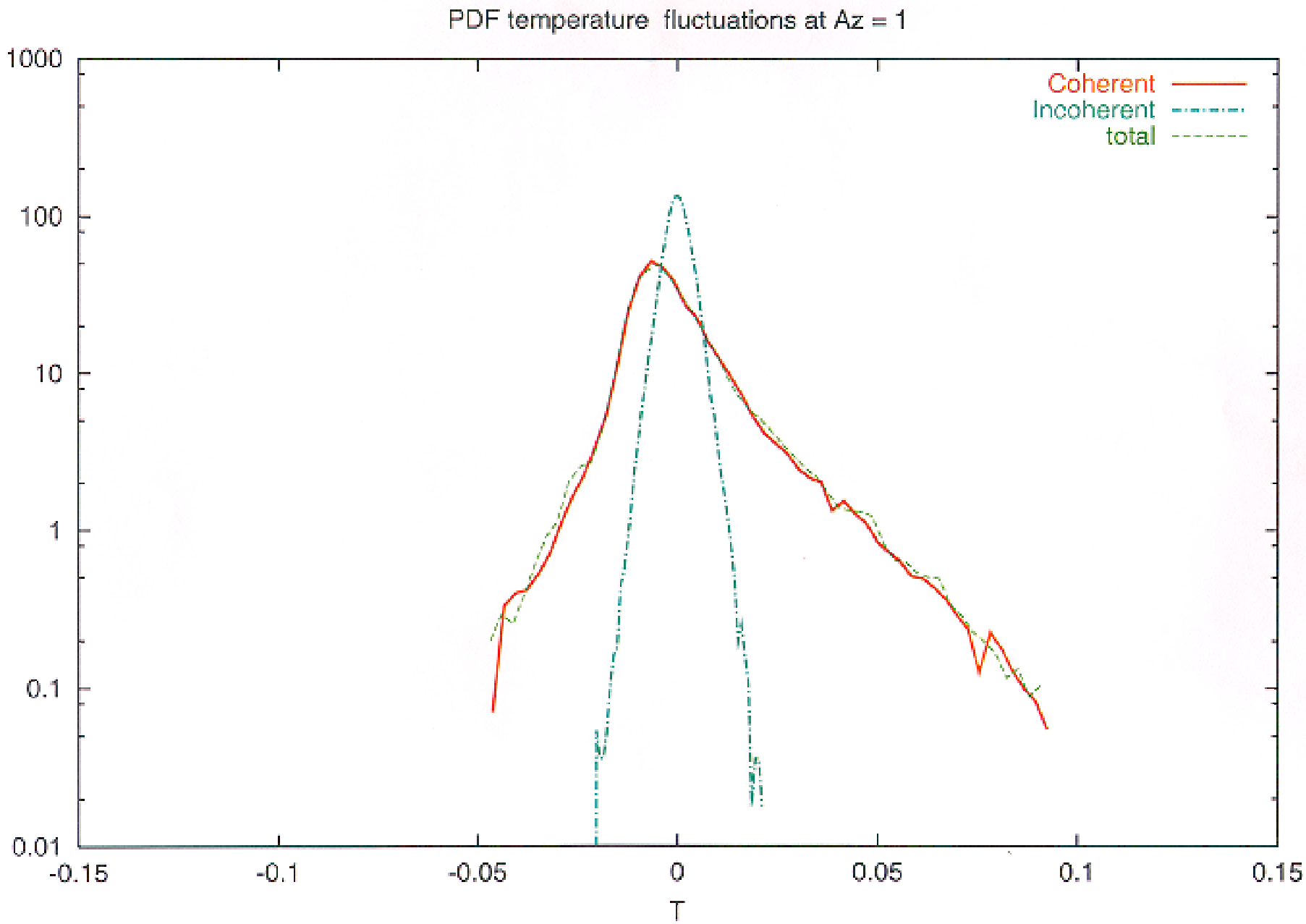

Wavelet Analysis

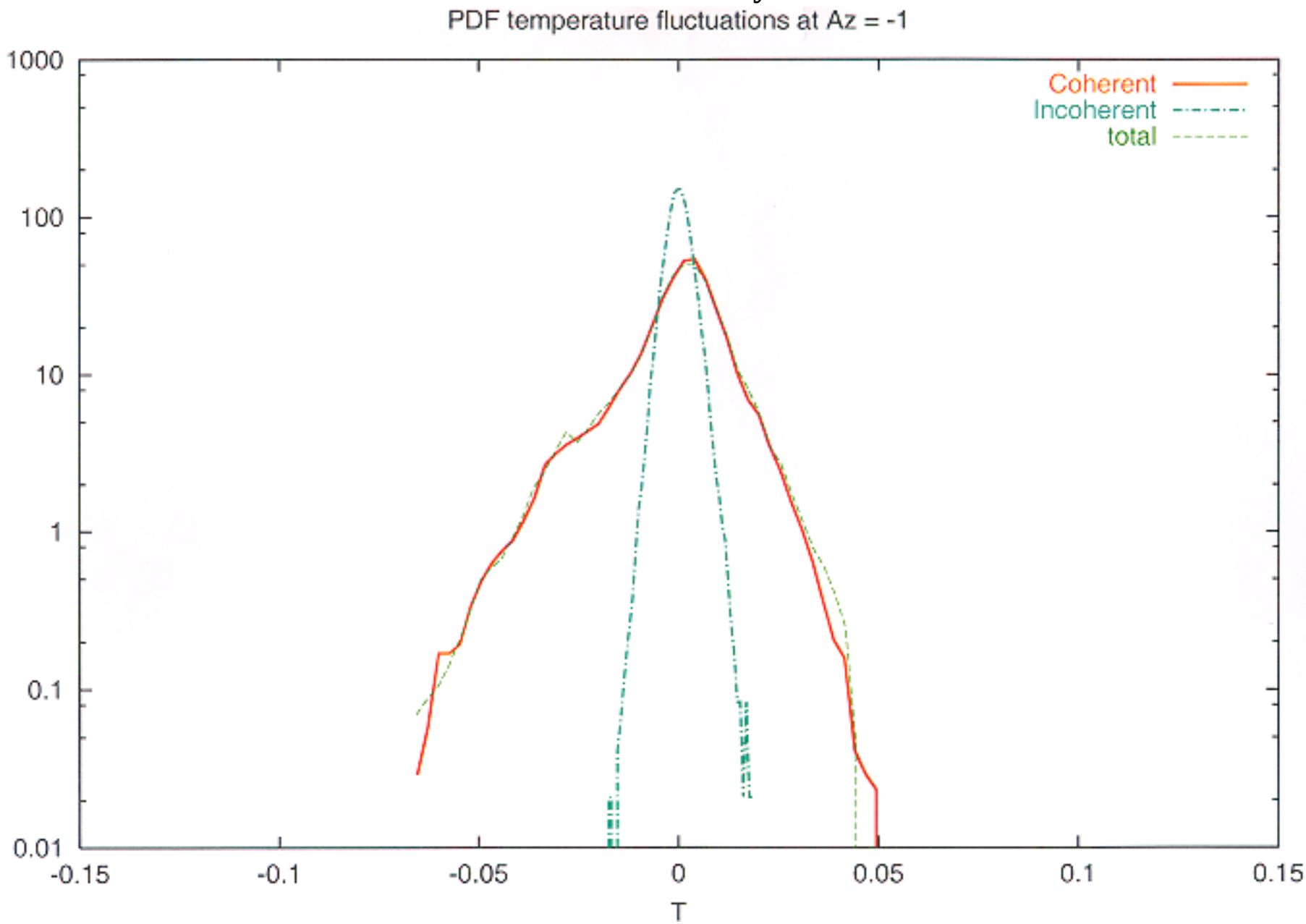

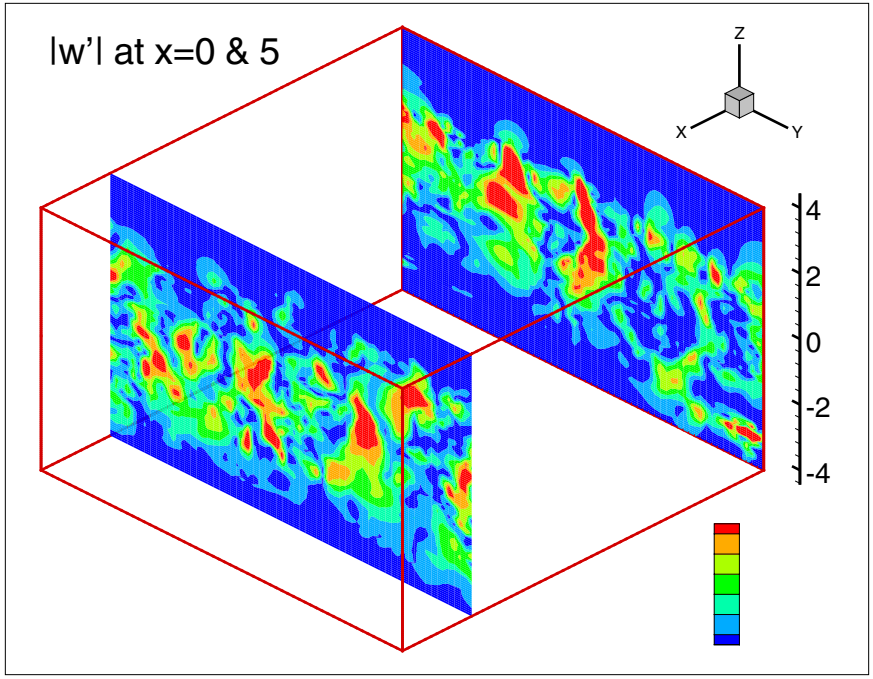
|w'| at x=0 & 5
Z
X
Y
4
2
0
-2
-4

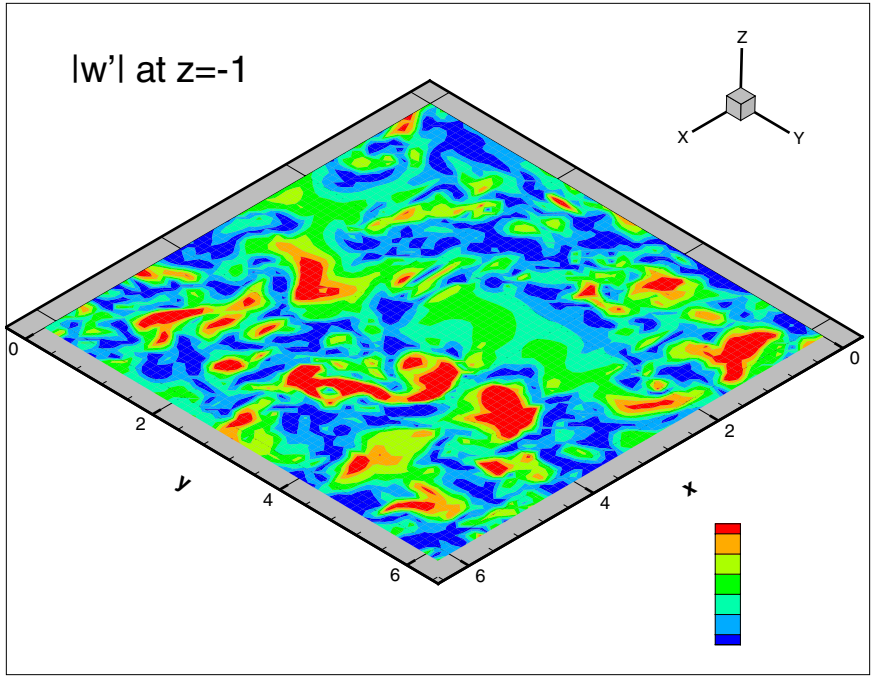
|w'| at z=-1
Z
X
Y
0
2
4
6
y
0
2
4
6
x

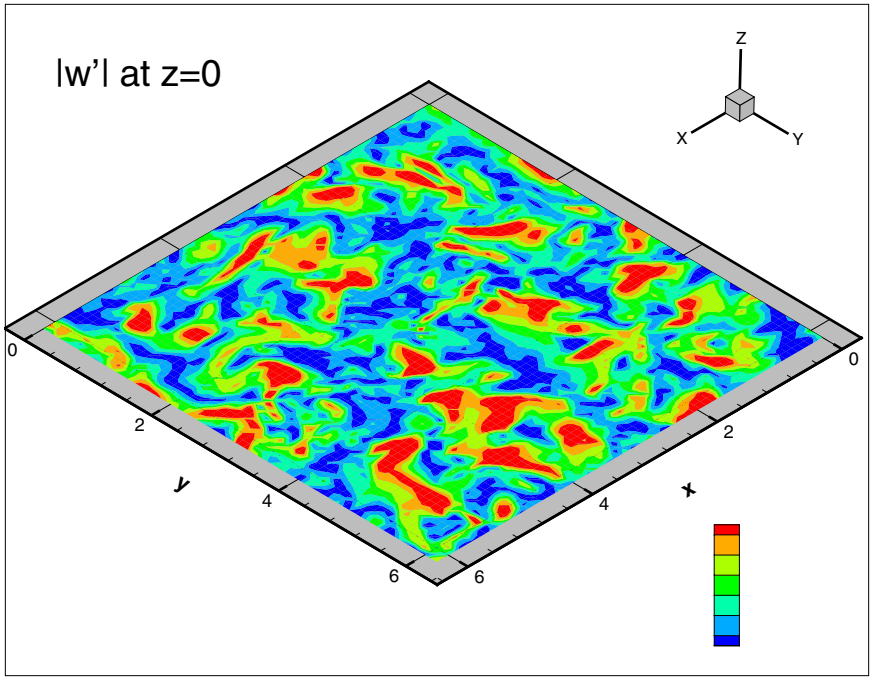
|w'| at z=0
Z
X
Y
0
2
4
6
y
0
2
4
6
x

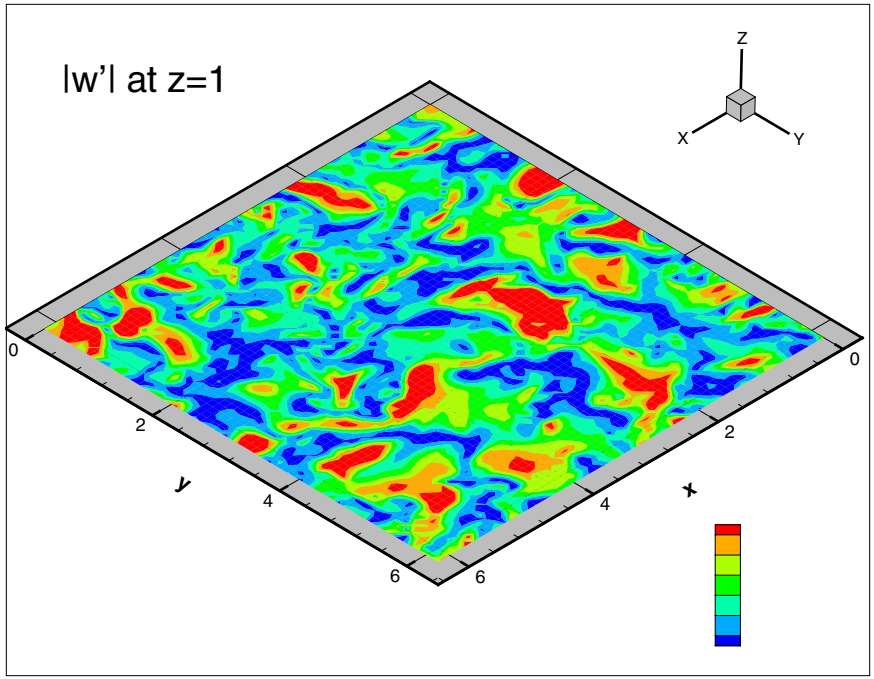
|w'| at z=1
Z
X
Y
0
2
4
6
y
0
2
4
6
x

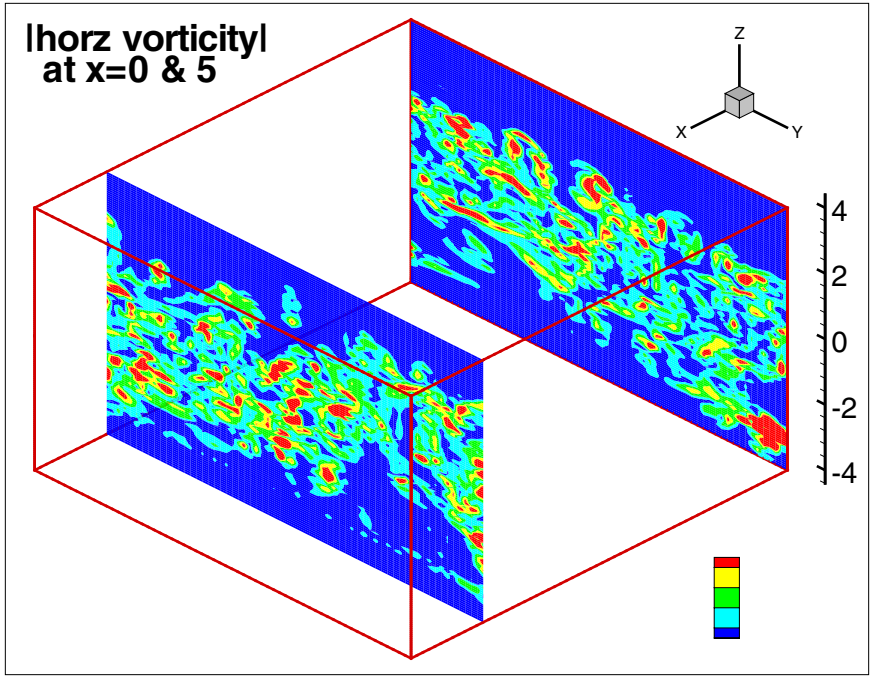
|horz vorticity|
at x=0 & 5
Z
X
Y
4
2
0
-2
-4

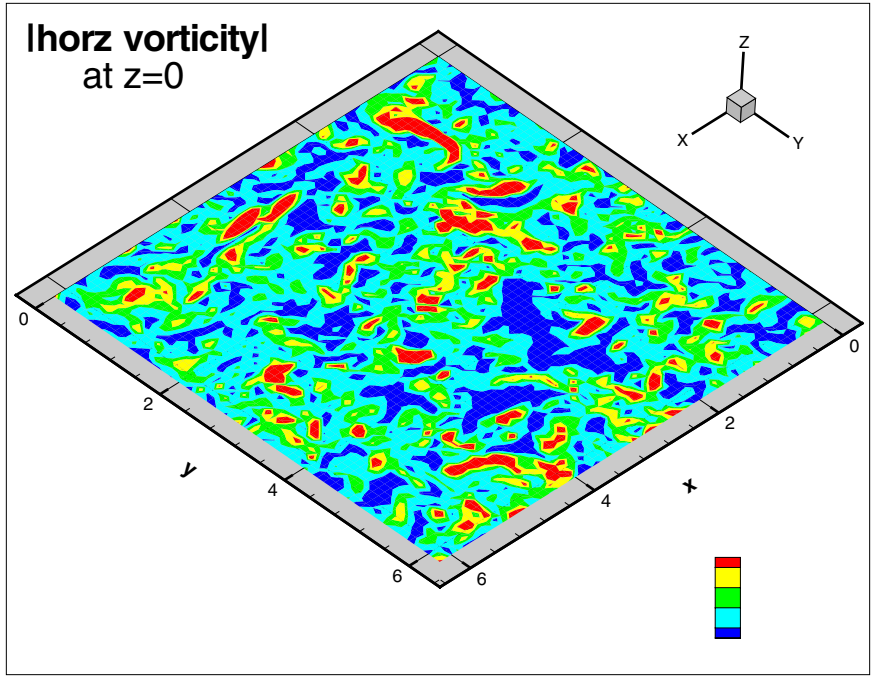
|horz vorticity|
at z=0
Z
X
Y
0
2
4
6
y
0
2
4
6
x

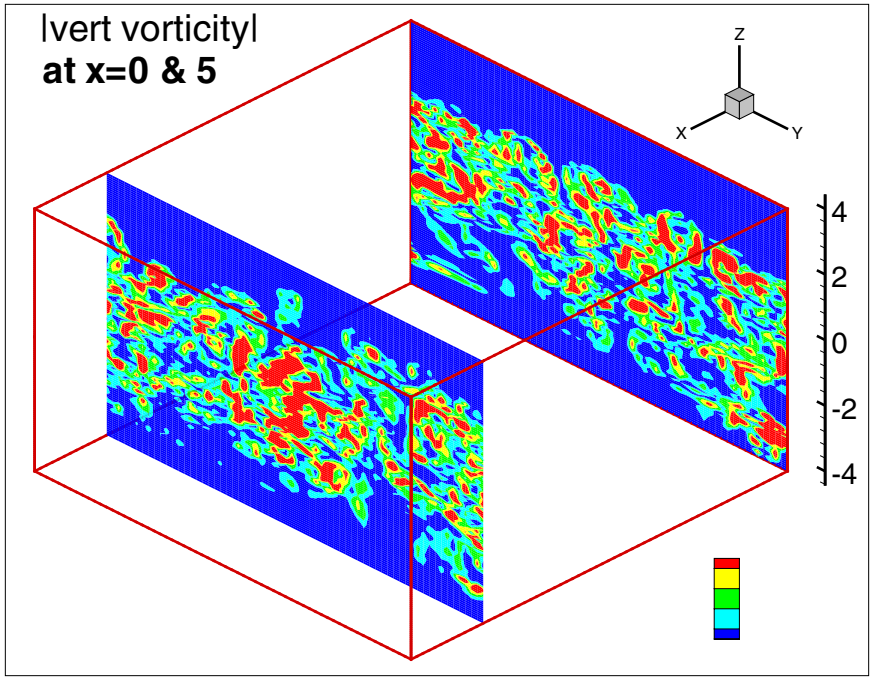
|vert vorticity|
at x=0 & 5
Z
X
Y
4
2
0
-2
-4

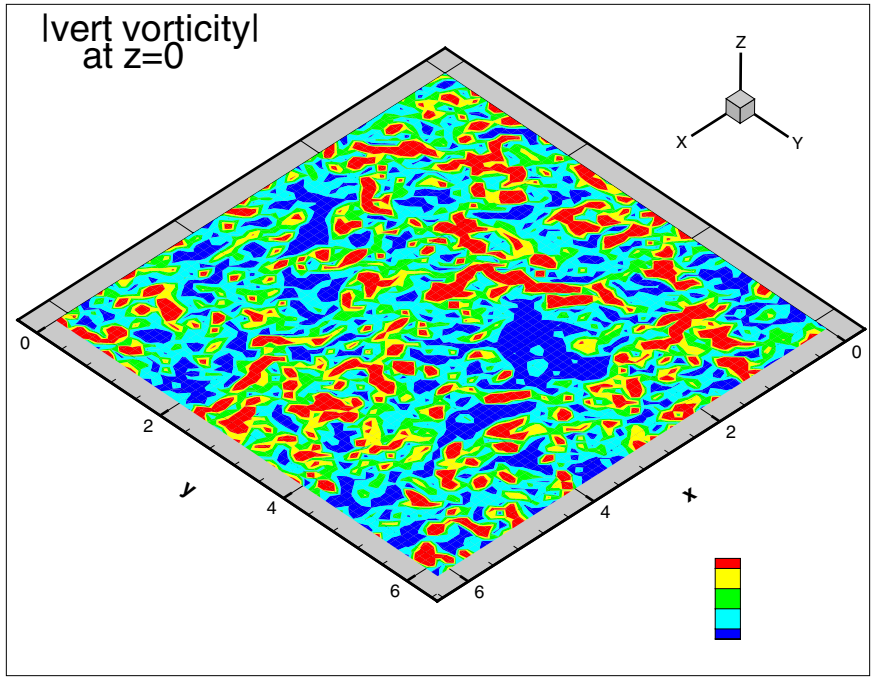
|vert vorticity|
at z=0
Z
X
Y
0
2
4
6
y
0
2
4
6
x

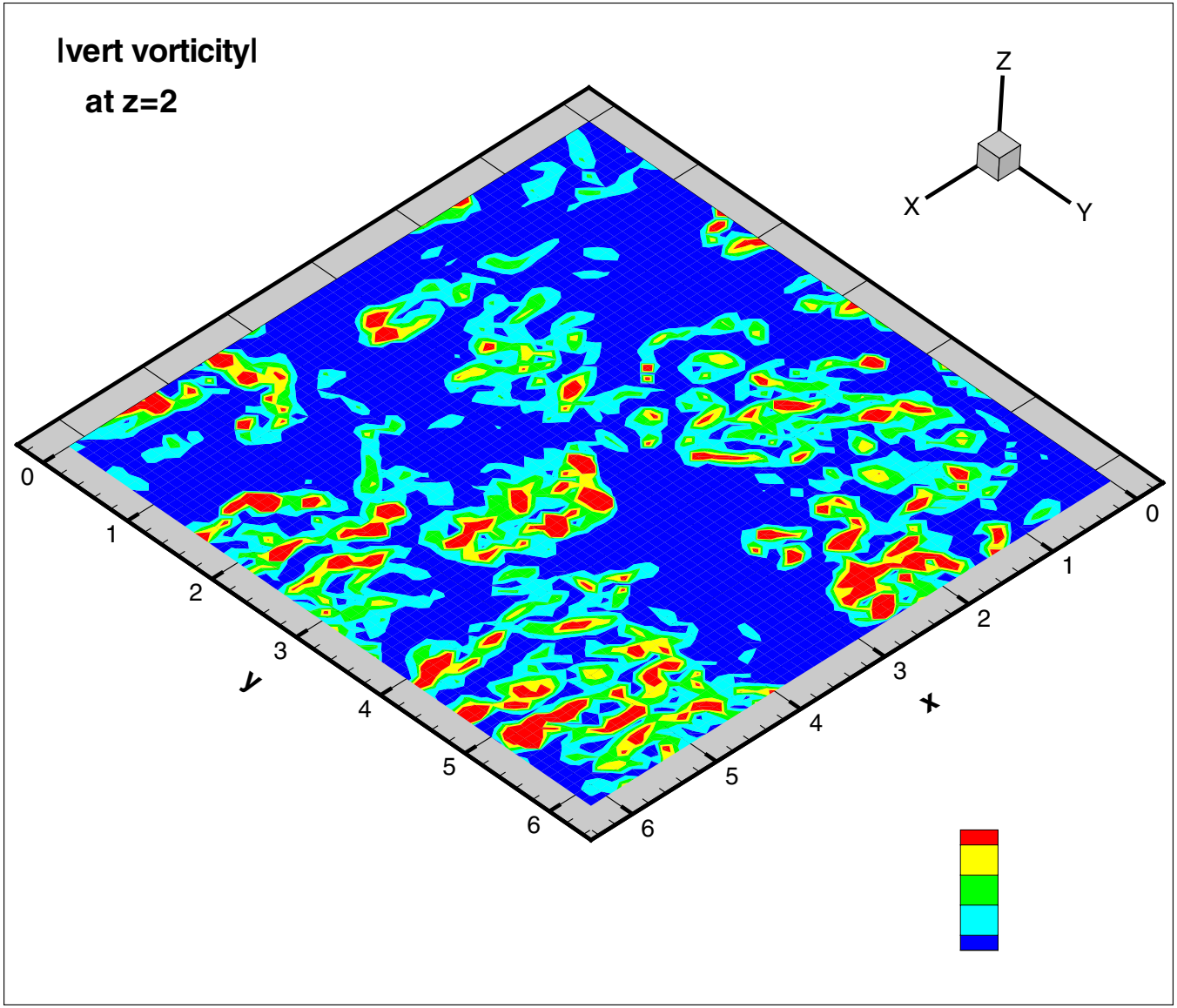
|vert vorticity|
at z=2
Z
X
Y
0
1
2
3
4
5
6
y
0
1
2
3
4
5
6
x

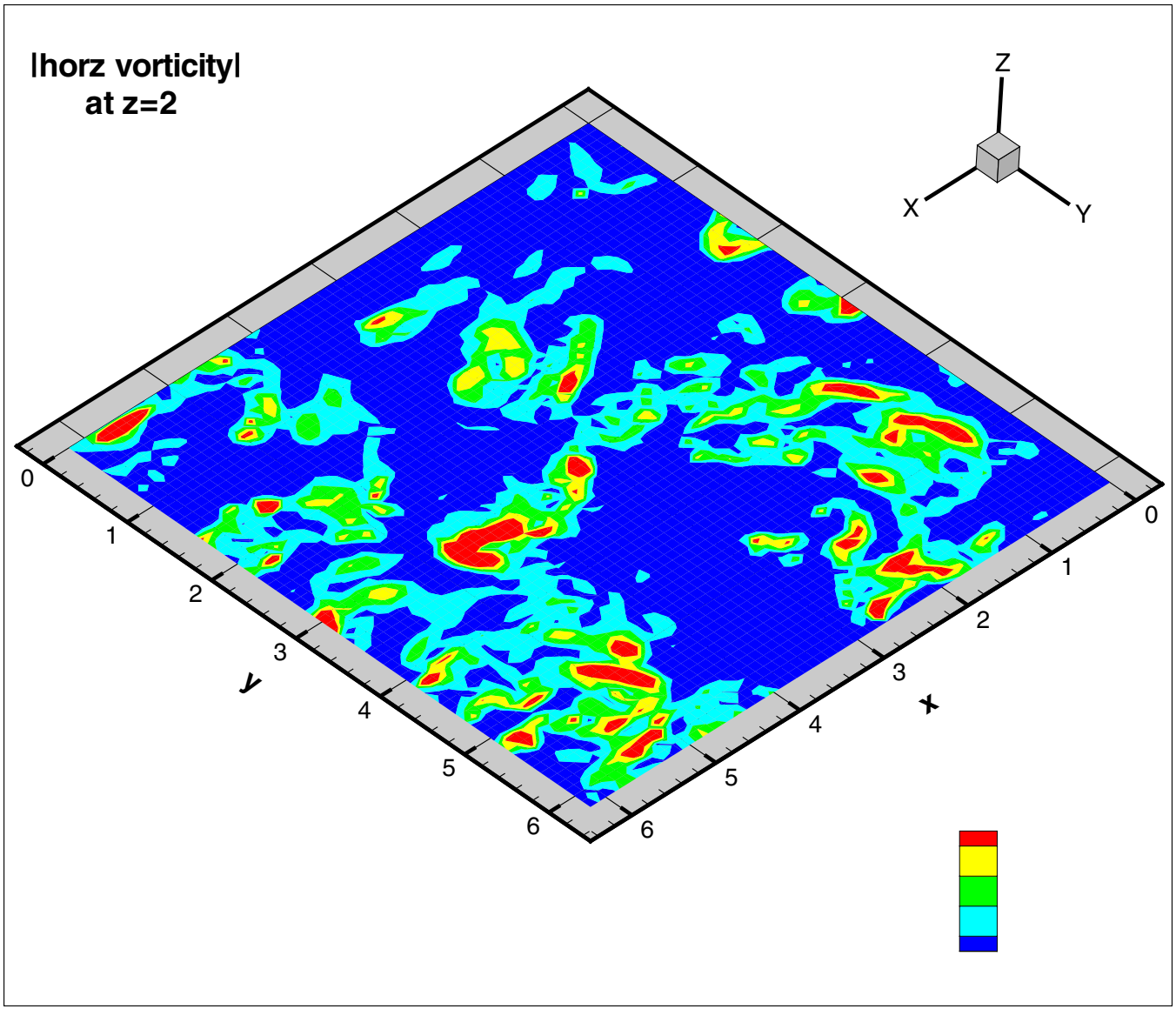
|horz vorticity|
at z=2
Z
X
Y
0
1
2
3
4
5
6
y
0
1
2
3
4
5
6
x

Velocity projection on a vertical plane, the contours are temperature fluctuation - high resolution case.

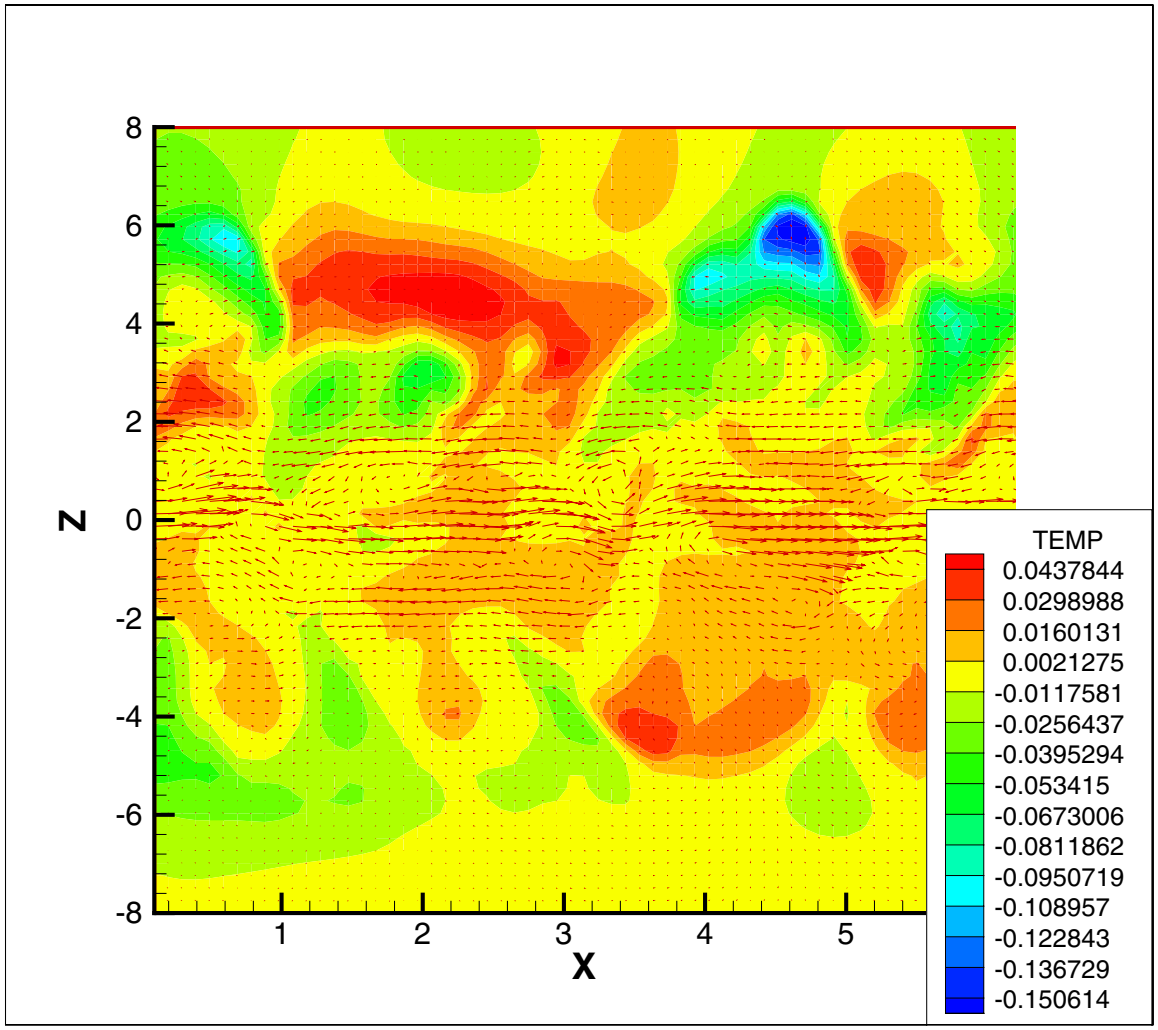

Local Gradient Richardson Number - high resolution case.

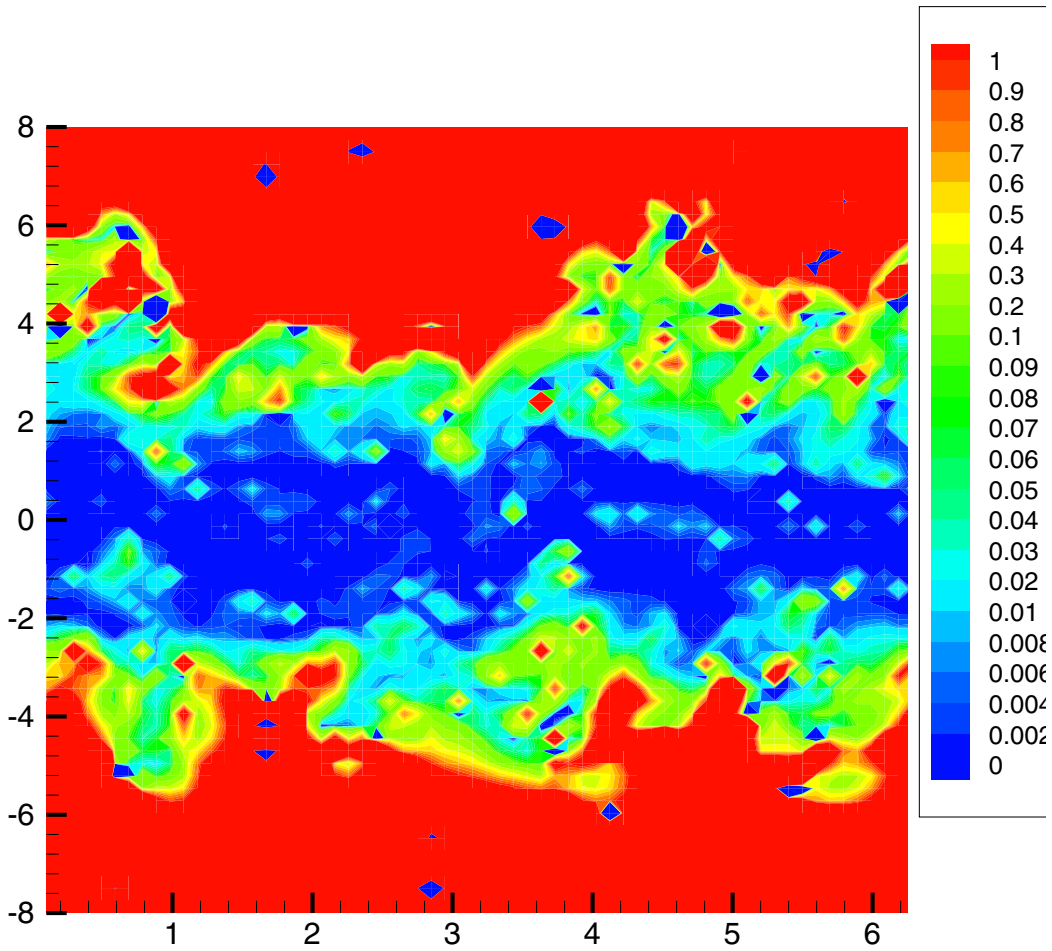

2. The AFGL Radiosonde Model for C_n^2 (Above Boundary Layer)

2.1 Basic Concepts

The key equation for the AFGL model is:

$$C_n^2 = 2.8 M^2 L^{4/3} \tag{1}$$

where:

$$M^2 = \left[\left(\frac{79 \times 10^{-6} P}{T^2}\right)\left(\frac{dT}{dz} + \gamma\right)\right]^2 \tag{2}$$

and where T is absolute atmospheric temperature in °K, P is pressure in mb, γ is the dry adiabatic lapse rate of 9.8 x 10^{-3} °K/m, and z is the height above ground. (Tatarski, 1961, and Dewan, 1980). Radiosondes give us P and T directly, but L in Eq. (1) is "the outer length," that is, the largest scale of inertial range turbulence. This is the unknown that our model will supply. A good rule of thumb, based on information in Pond et al. (1963) and Tennekes and Lumley (1972), is that L would be of the order of 0.1 times the thickness of a turbulent layer. In principle this could be used in the future as an adjustable parameter (that is, one could use values other than 0.1) but at present using other values seems to be unnecessary.

PL-TR-93-2043
Environmental Research Papers, No. 1121

A MODEL FOR C_n^2 (OPTICAL TURBULENCE) PROFILES USING RADIOSONDE DATA

E. M. Dewan
R. E. Good
R. Beland
J. Brown

1 March 1993

Approved for public release; distribution unlimited

PHILLIPS LABORATORY
Directorate of Geophysics
AIR FORCE MATERIEL COMMAND
HANSCOM AIR FORCE BASE, MA 01731-3010

SCALES OF TURBULENCE

$L_K = \left(\frac{\nu^3}{\varepsilon}\right)^{\frac{1}{4}}$ **— Kolmogorov scale**

$L_b = \frac{\sigma_w}{N}$ **— Buoyancy scale**

σ_w **— r.m.s. vertical velocity** w **fluctuation**

$L_e = \frac{\sigma_\theta}{\left\langle \left| \frac{d\theta}{dZ} \right| \right\rangle}$ **— Ellison scale**

$L_O = \left(\frac{\varepsilon}{N^3}\right)^{\frac{1}{2}}$ **— Ozmidov scale**

L_O **is the scale at which eddies have enough energy to be unstable (or overturn) in the stable buoyancy gradient** N^2**.**

Outer Scales of Turbulence

$$L_s = \frac{q}{\left\langle \left| \frac{dU}{dz} \right|^2 \right\rangle^{1/2}}$$ – shear scale

$$q^2 = u'^2 + v'^2 + w'^2$$

$$L_t = \left(\frac{\varepsilon}{S^3} \right)^{1/2}$$ – Tatarski scale

$$S = \left\langle \left| \frac{dU}{dz} \right|^2 \right\rangle^{1/2}$$ – shear

$$L_o = \left(\frac{\varepsilon}{N^3} \right)^{1/2}$$ – Ozmidov scale
N-Brunt-Väisäla

$$L_b = \frac{q}{N}$$ – buoyancy scale
(Deardorff scale)

$$\frac{L_s^2}{L_b^2} = \frac{N^2}{\left\langle \left| \frac{dU}{dz} \right|^2 \right\rangle}$$ – gradient Richardson number ($\mathrm{Ri_g}$)

$$\frac{L_t^2}{L_o^2} = \frac{N^3}{S^3} = \mathrm{Ri_g}^{3/2}$$

Vertical Profile of Reynolds number based on $L_d(= q^3/\epsilon)$ scale - high resolution case.

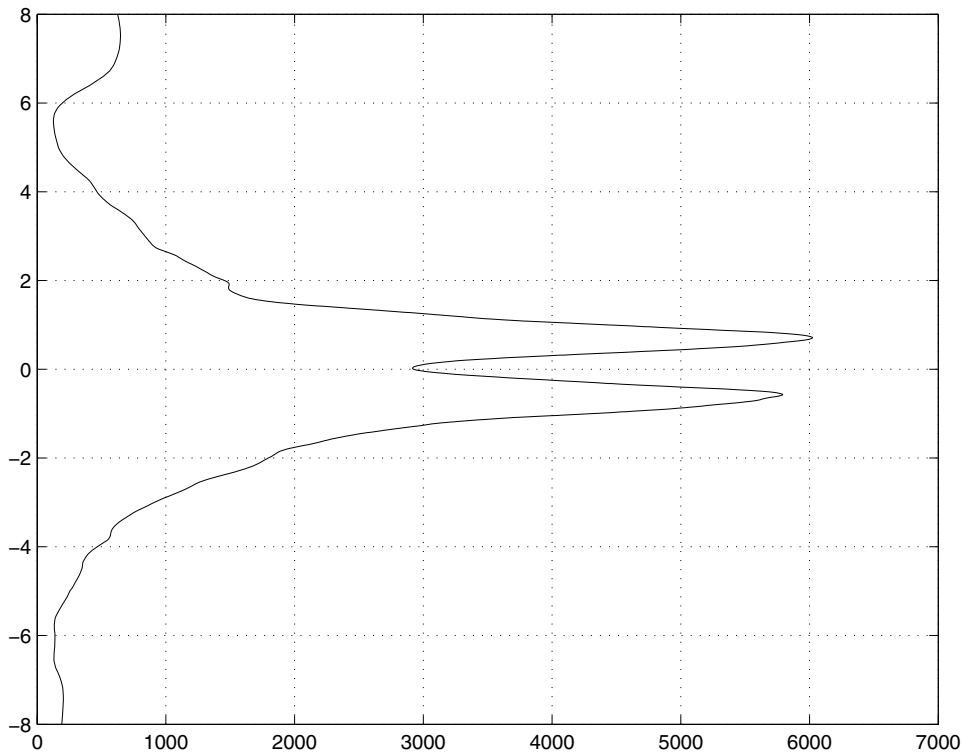

High Resolution Case

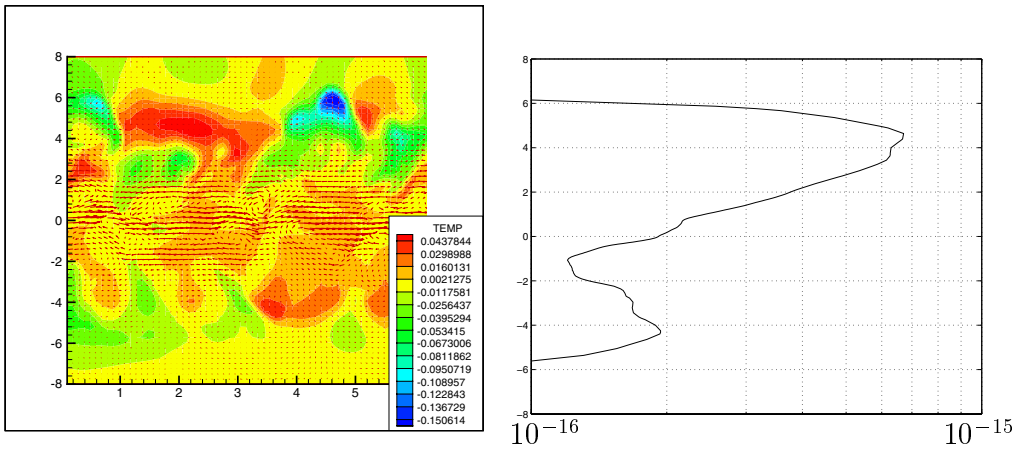

Figure 1: Contours of temperature fluctuation (left) and logarithmic plot of C_N^2 (right).

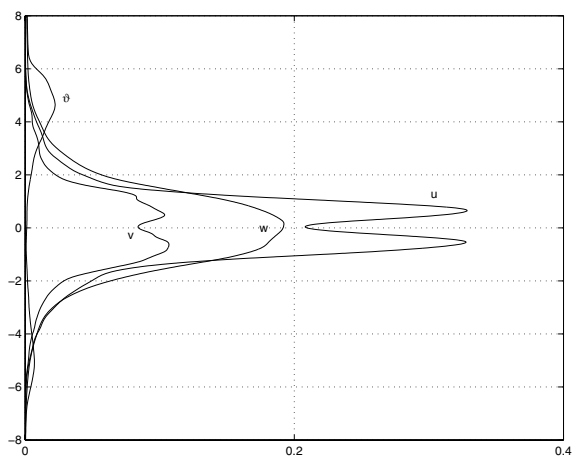

Figure 2: Velocities and temperature variances.

Radio Science, Volume 36, Number 1, Pages 137–149, January–February, 2001

Persistent layers of enhanced C_N^2 in the lower stratosphere from VHF radar observations

G. D. Nastrom

St. Cloud State University, St. Cloud, Minnesota

F. D. Eaton

Air Force Research Laboratory, Kirtland Air Force Base, New Mexico

Abstract. Seasonal climatologies of persistent layers of enhanced refractive index structure parameter C_N^2 were developed for the lower stratosphere from VHF radar observations at White Sands Missile Range, New Mexico, for the period January 1991 to September 1996. Knowledge of the nature of enhanced refractivity layers is of high interest to the atmospheric sciences, propagation, and remote sensing communities. The layers reported have C_N^2 enhanced at least 7 dB above the background continuously for at least 11 hours and migrate vertically no more than one radar range gate (150 m) over 1 hour. The cumulative frequency of the lengths (11–37 hours) of the 259 persistent layers identified shows that 25% of the layers last over 17 hours. Comparisons of profiles of wind speeds, variances of the wind components, vertical shear of the horizontal wind, Doppler spectral width, temperature, Brunt-Vaisala frequency, and Richardon's number for times with and without persistent layers at 17 km show that wind speed at 5.6 km in addition to spectral width, wind shear, and vertical velocity variances at 17 km are stronger during enhanced layer episodes than during nonlayer periods. Possible sources for the persistent layers are suggested, and the shortcomings of each hypothesis are discussed. Several case studies of radiosonde ascents during persistent layers give no obvious indication of the source of these layers.

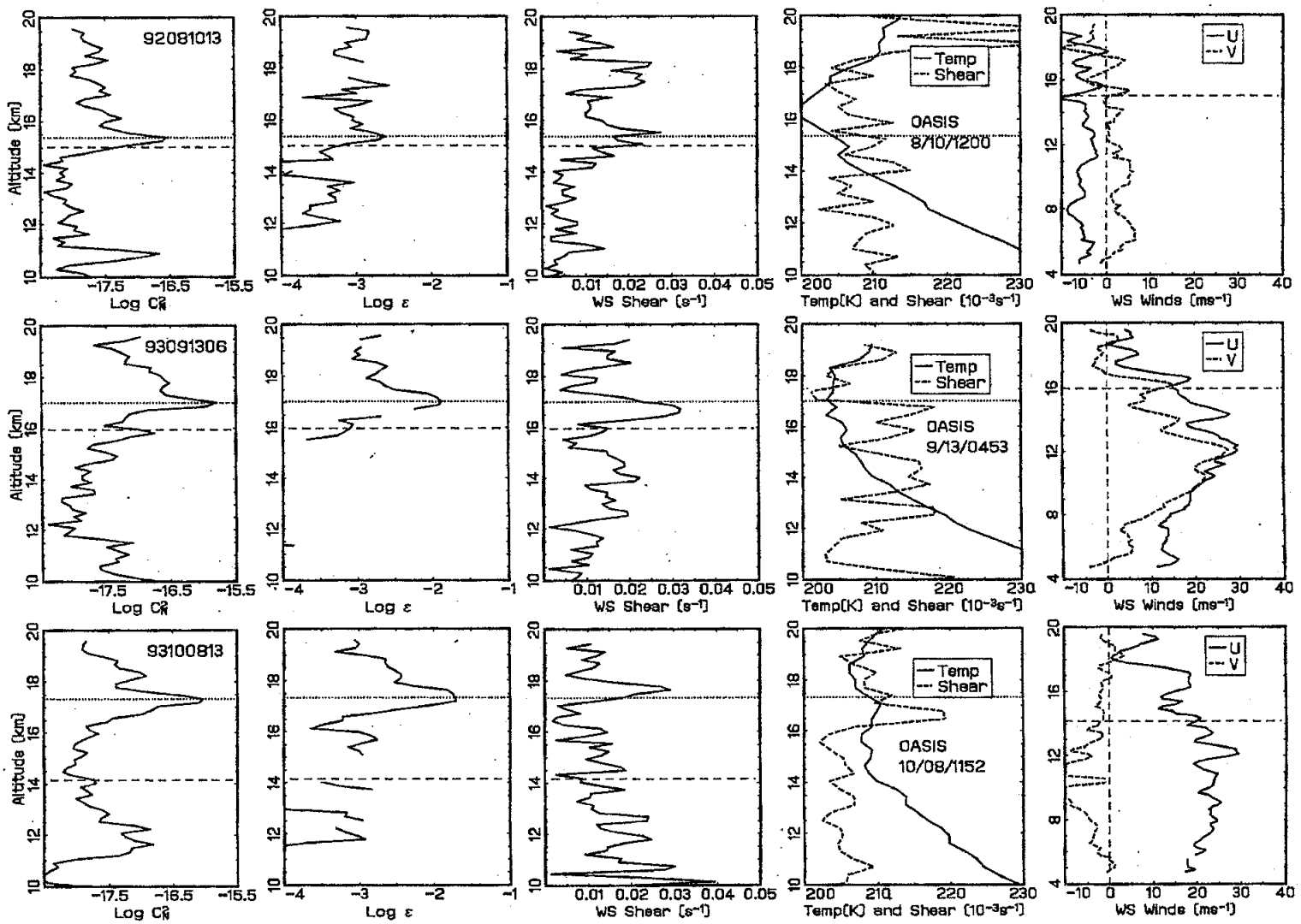

Figure 9. Profiles of hourly median C_N^2, ε, u, v, and wind shear based on WS radar data for August 10, 1992, 1300 UT (upper row), September 13, 1993, 0600 UT (center row), and October 8, 1993, 1300 UT (lower row), plus temperature and wind shear based on radiosondes launched at WS at the times indicated. A dashed line is entered at the height of the tropopause interpolated in time from the El Paso soundings. A dotted line indicates the level of the maximum C_N^2. The balloon-based shears have been multiplied by 10^3 and then shifted 200.

Normalized horizontal heat flux, $\langle u'\vartheta' \rangle$ (I) and Vertical heat flux, $\langle w'\vartheta' \rangle$ (II) - high resolution case.

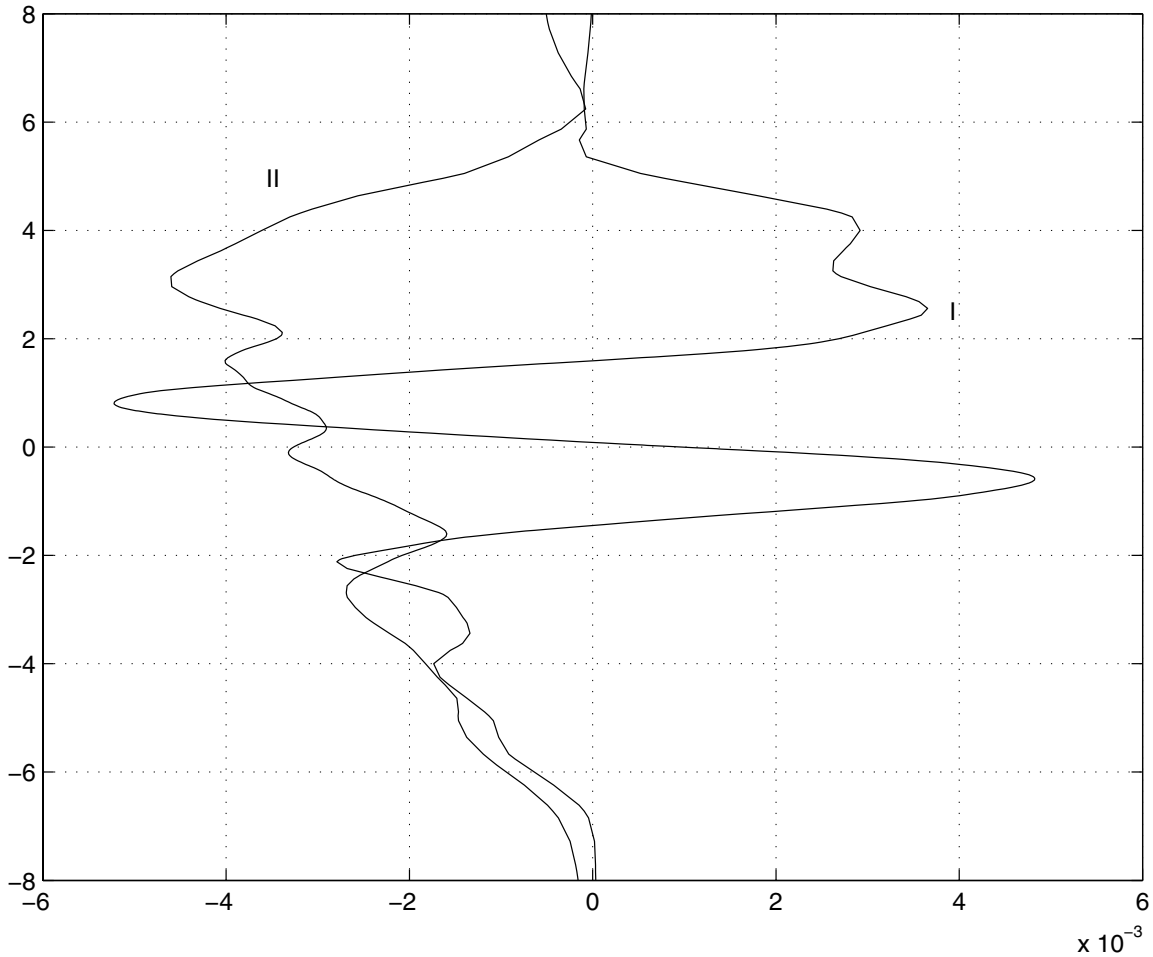

Normalized length scales - high resolution case.

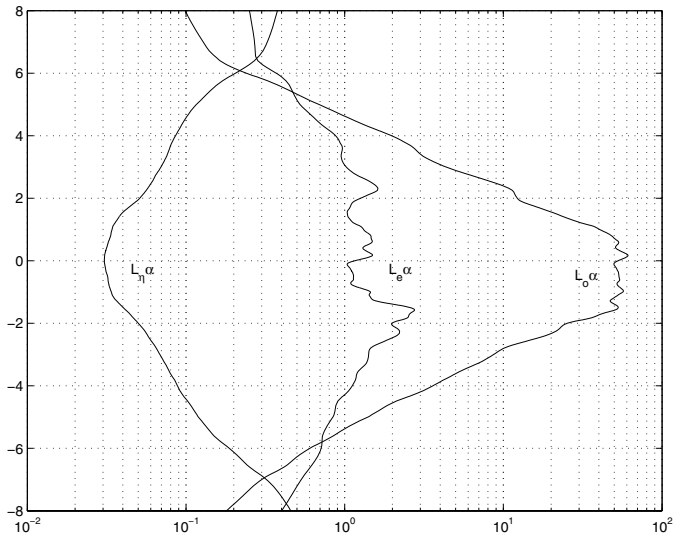

Figure 1: $L_\eta\alpha$, $L_e\alpha$, $L_o\alpha$

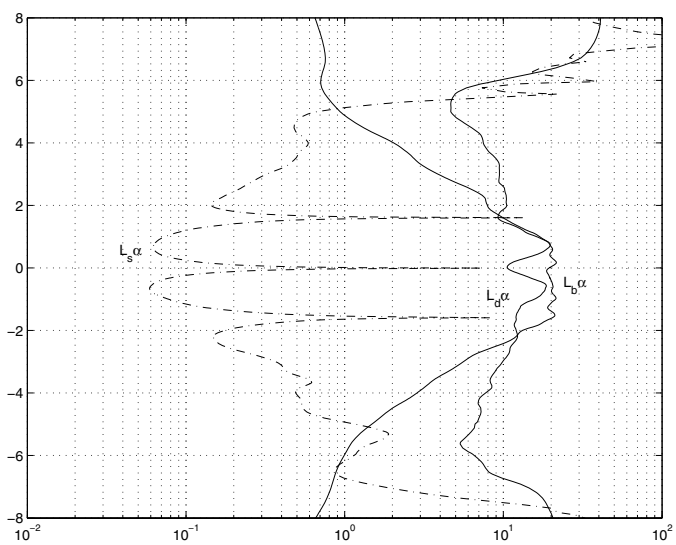

Figure 2: $L_s\alpha$, $L_d\alpha$ and $L_b\alpha$

Tatarskii scale (L_t) and Ozmidov scale (L_o) - high resolution case.

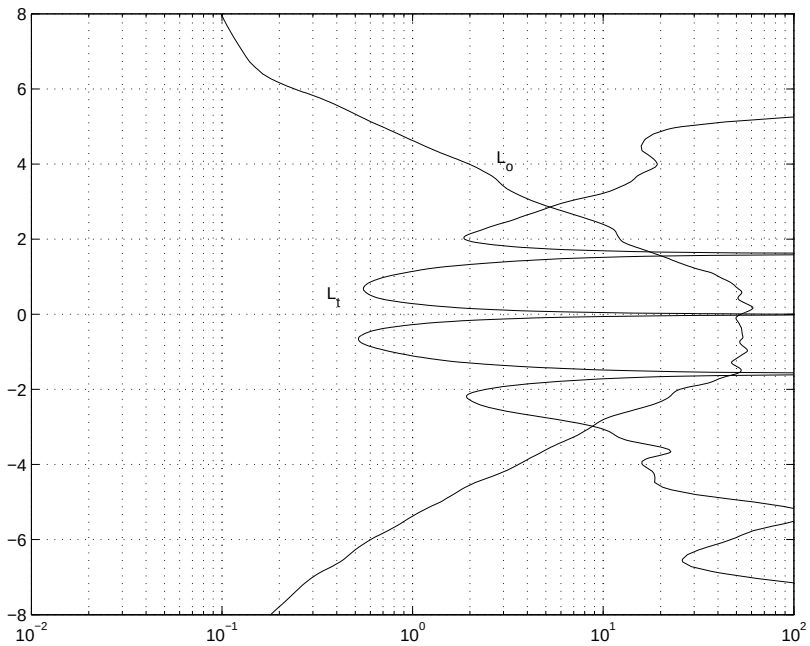

Ratio of length scales - high resolution case.

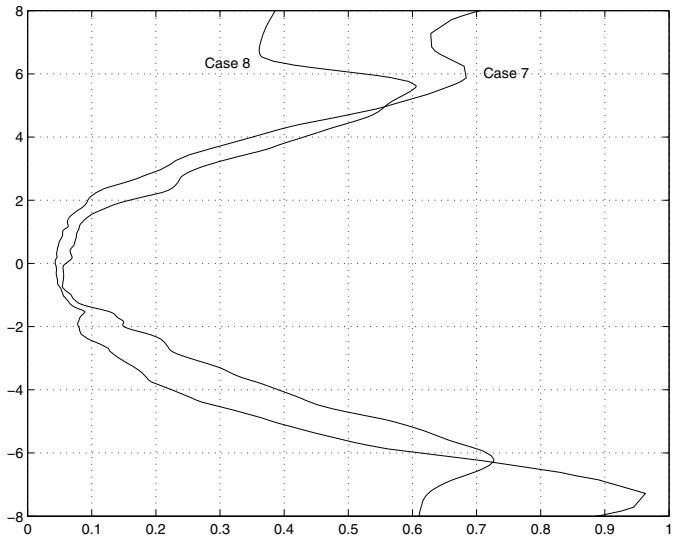

Figure 1: L_e/L_b

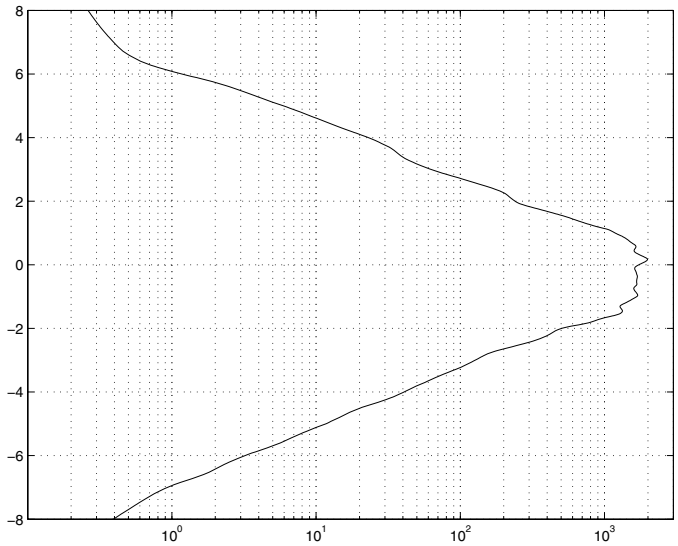

Figure 2: L_o/L_η

Jet Structure and Richardson Number

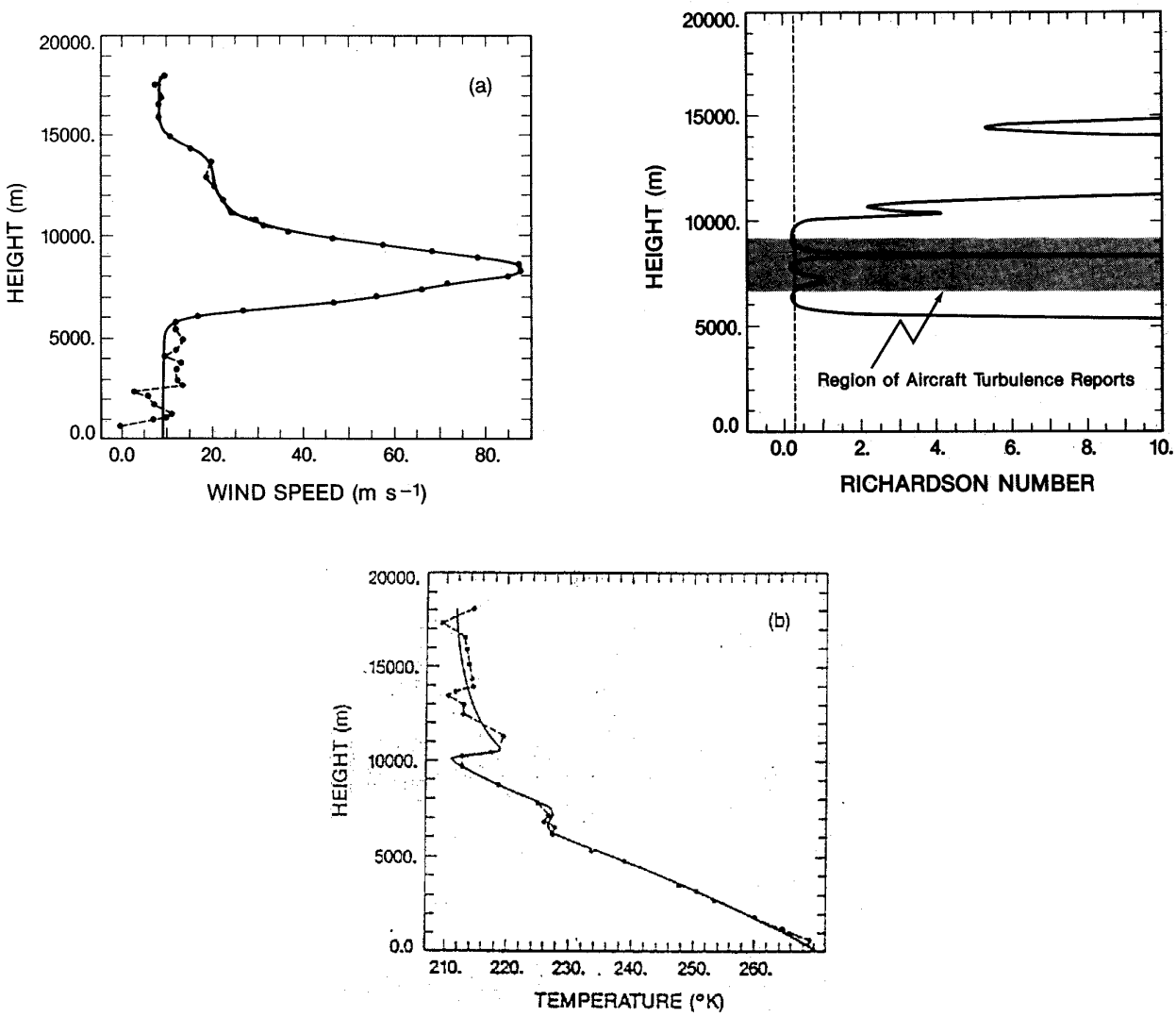

From Bedard, Canavero and Einaudi (1986)

Richardson number
- from high resolution simulation (left) and observation of Bedard et. al.(right).

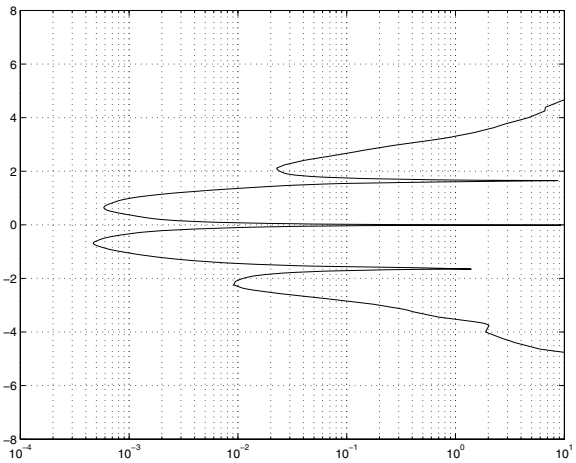

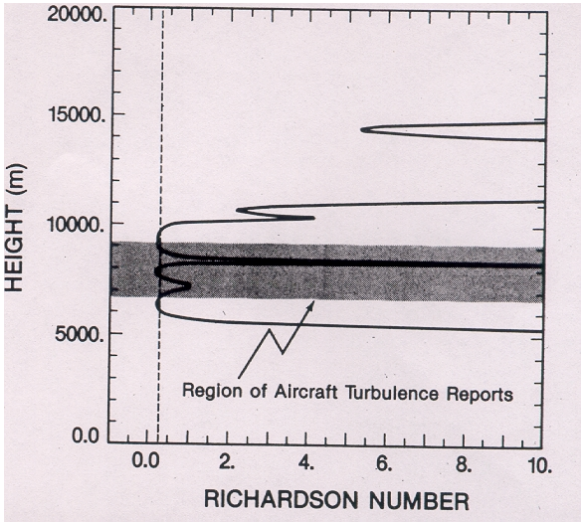

Ratio of Tatarski scale over Ozmidov scale
($L_t/L_o = Ri^{3/4}$) - high resolution case.

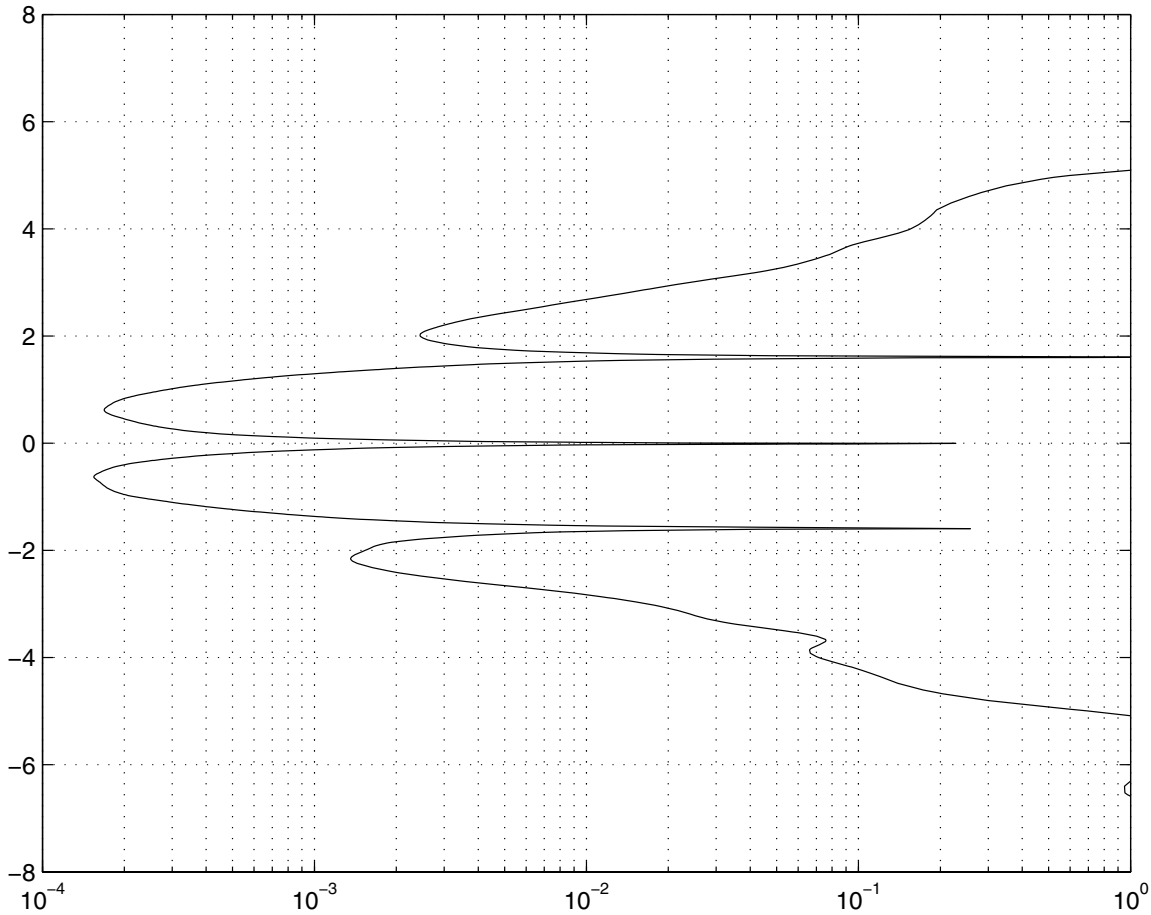

Ratio of Ozmidov scale over buoyancy Scale $\frac{L_o}{L_b}$ - High resolution case

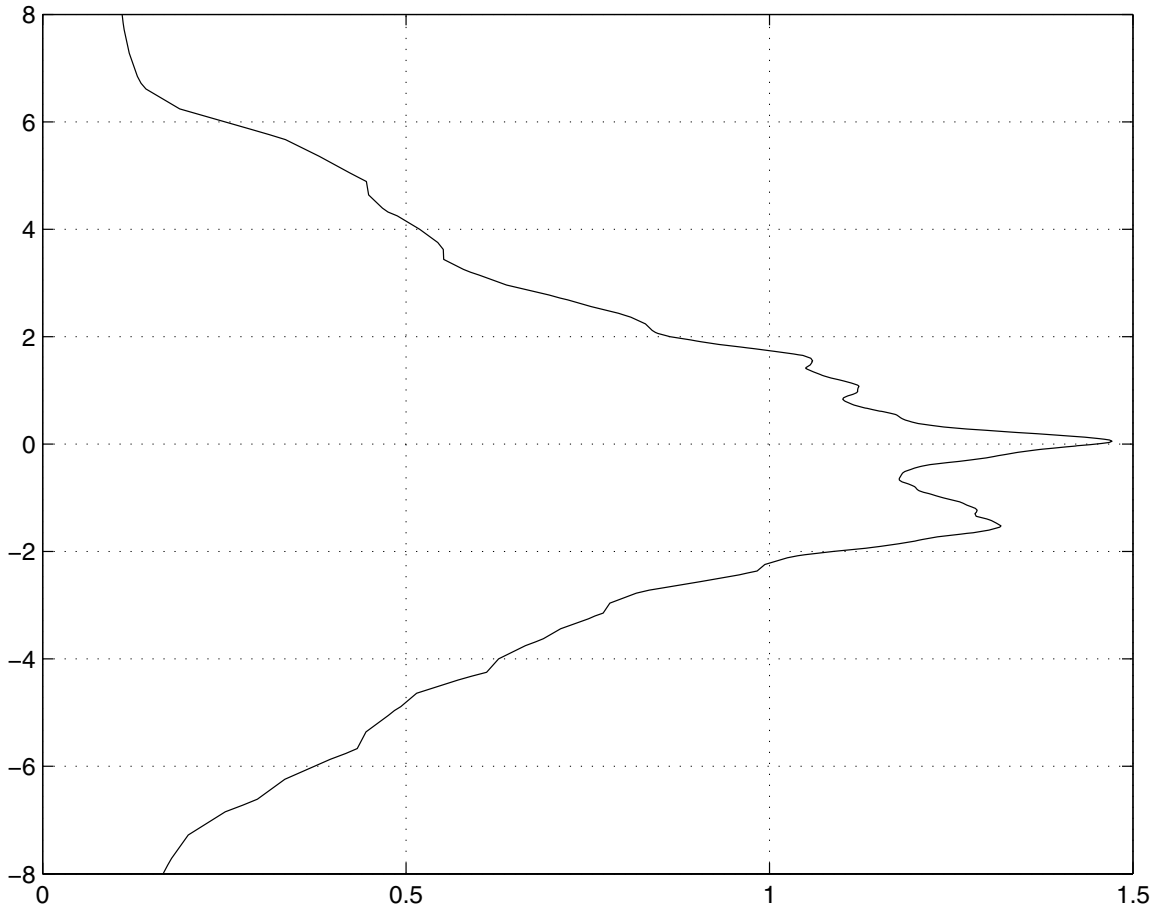

Turbulent Froude number $\left(Fr_t = \left(\frac{L_o}{L_e}\right)^{2/3}\right)$
- High resolution case

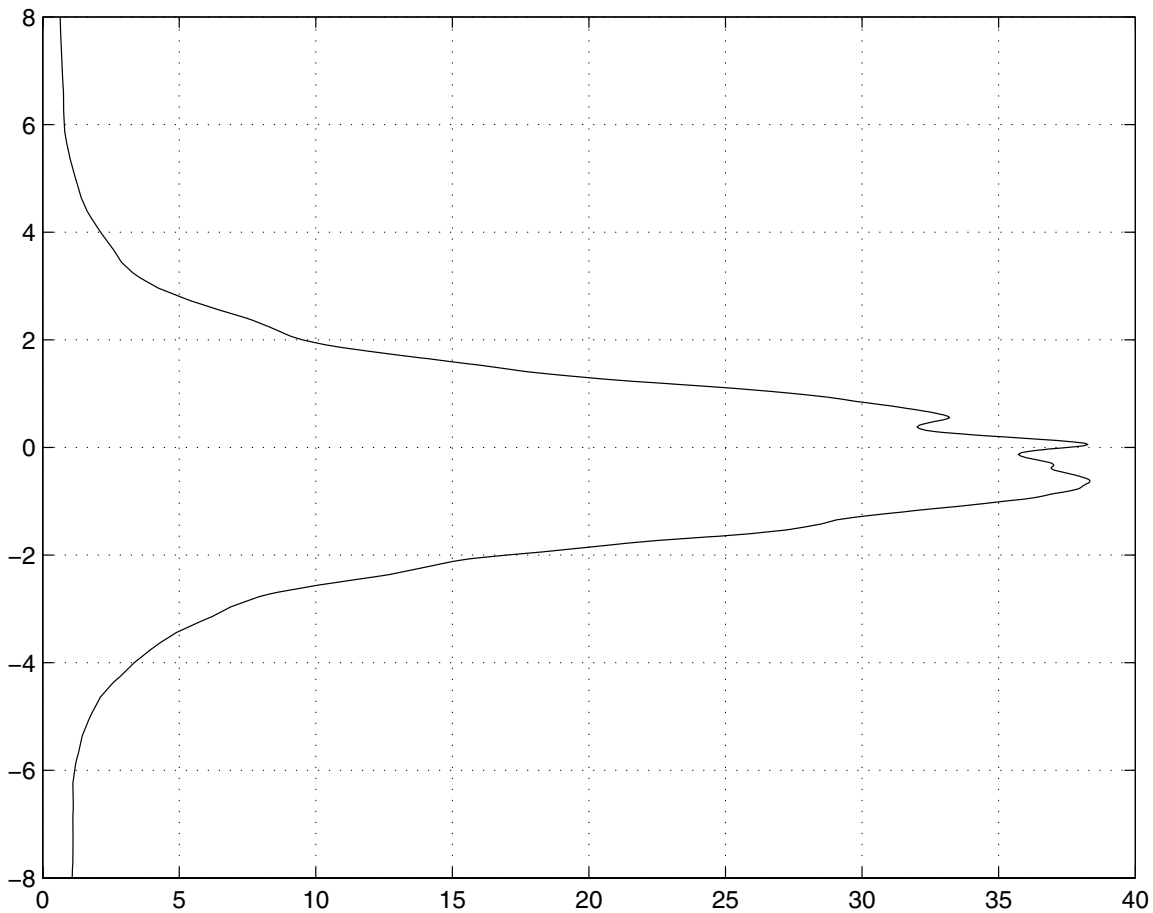

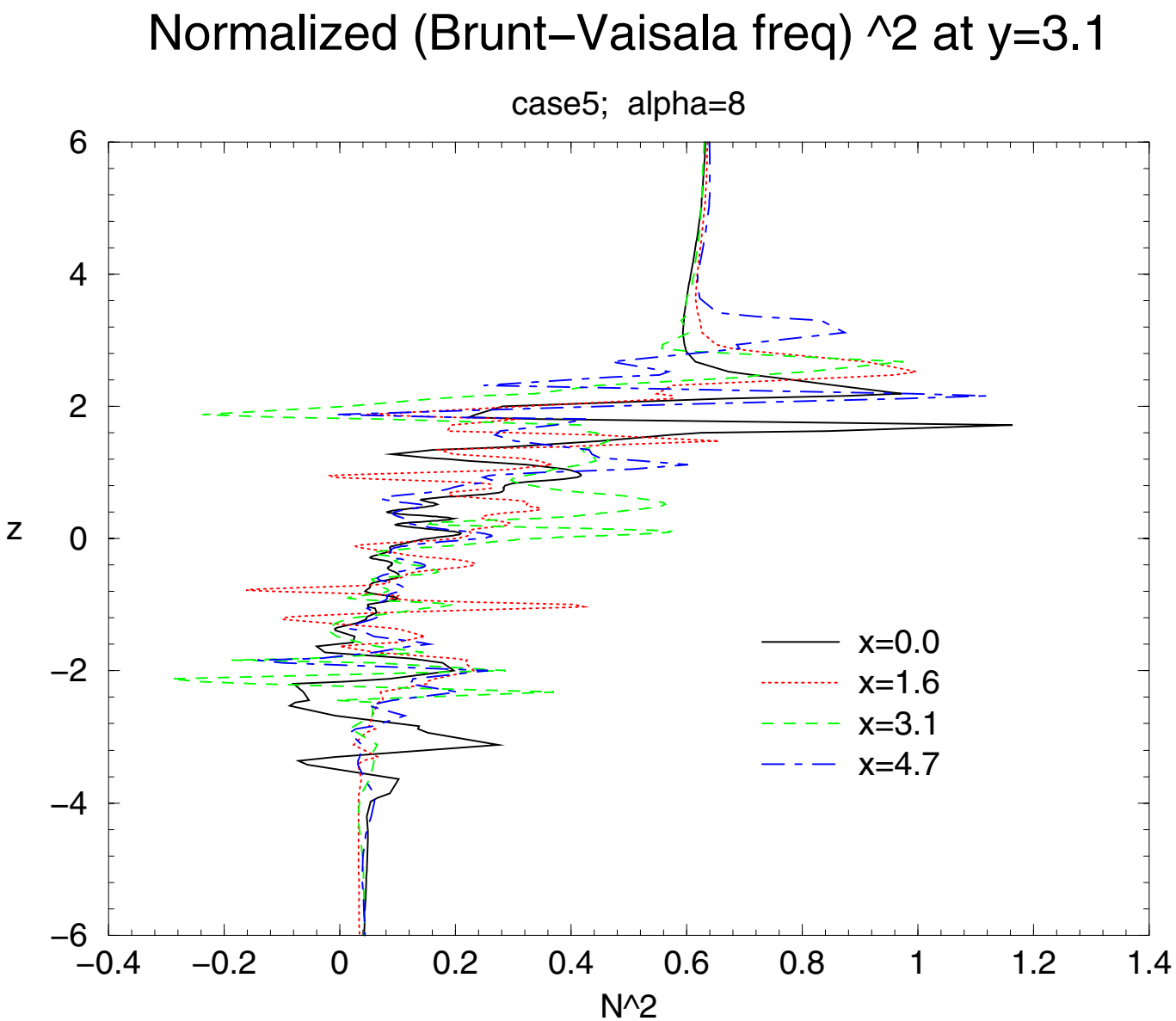
Normalized (Brunt–Vaisala freq) ^2 at y=3.1
case5; alpha=8
z
N^2
6
4
2
0
−2
−4
−6
−0.4
−0.2
0
0.2
0.4
0.6
0.8
1
1.2
1.4
x=0.0
x=1.6
x=3.1
x=4.7

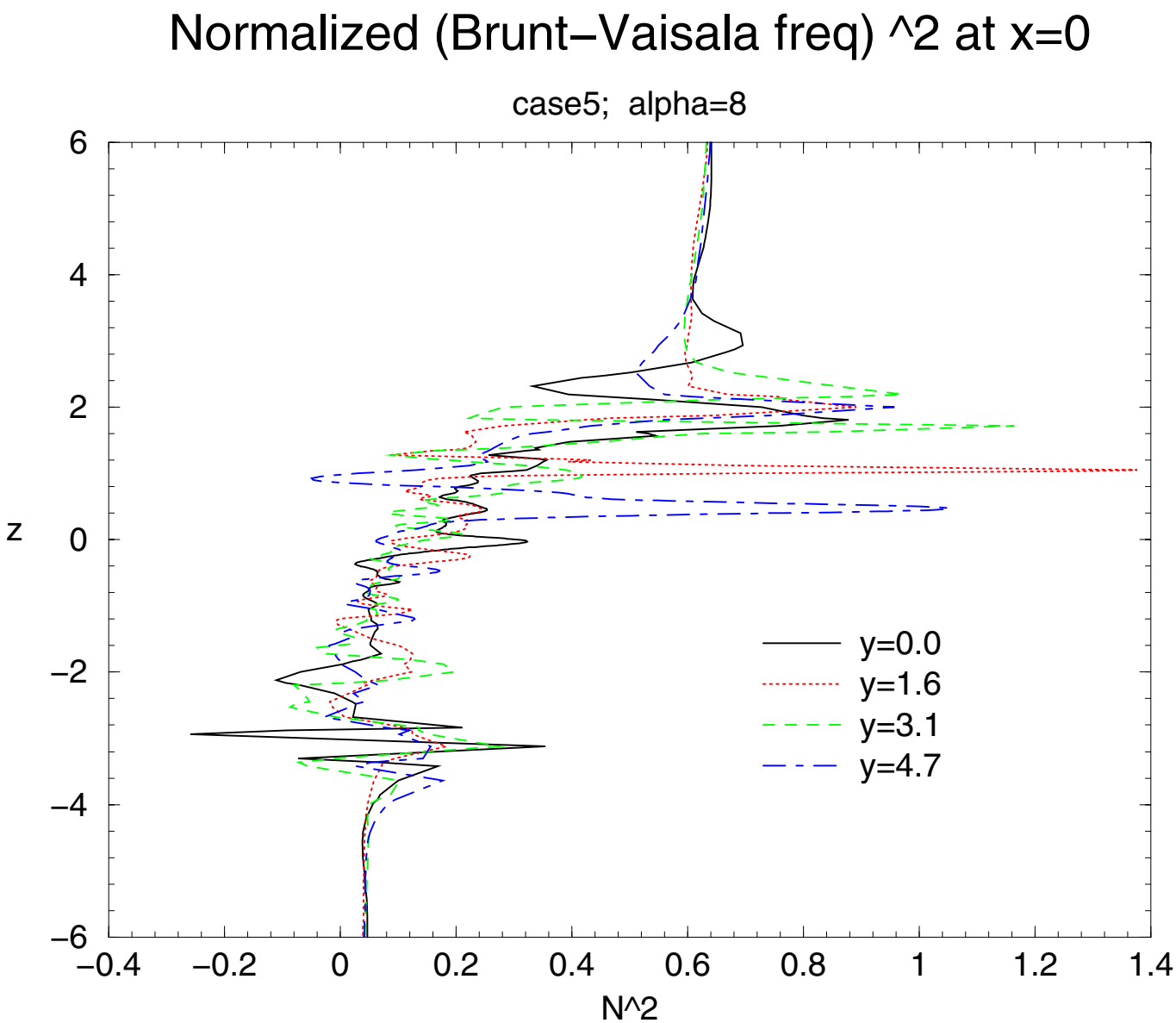
Normalized (Brunt–Vaisala freq) ^2 at x=0
case5; alpha=8
z
N^2
6
4
2
0
−2
−4
−6
−0.4
−0.2
0
0.2
0.4
0.6
0.8
1
1.2
1.4
y=0.0
y=1.6
y=3.1
y=4.7

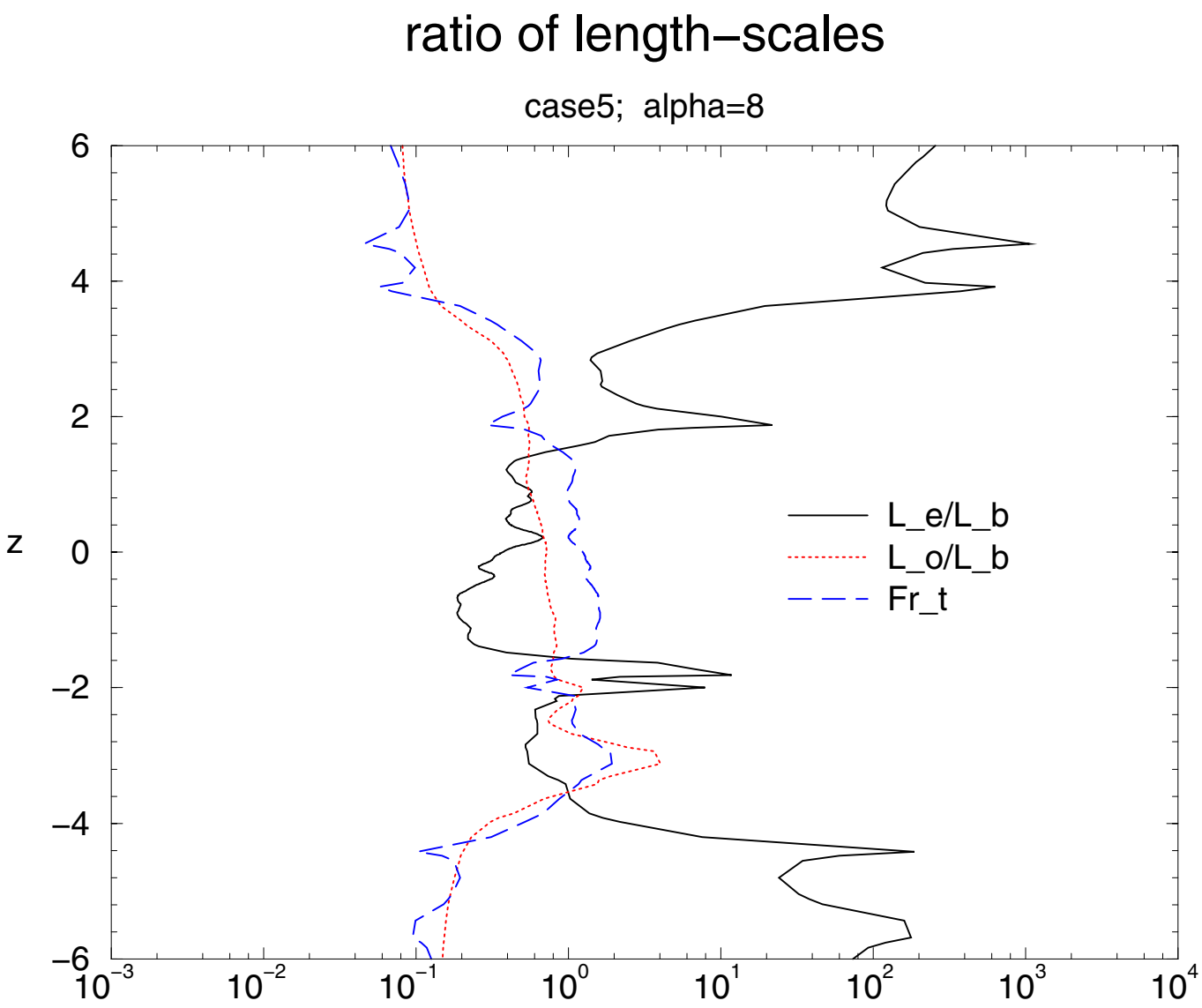
ratio of length−scales
case5; alpha=8
z
6
4
2
0
−2
−4
−6
10^{-3}
10^{-2}
10^{-1}
10^{0}
10^{1}
10^{2}
10^{3}
10^{4}
L_e/L_b
L_o/L_b
Fr_t

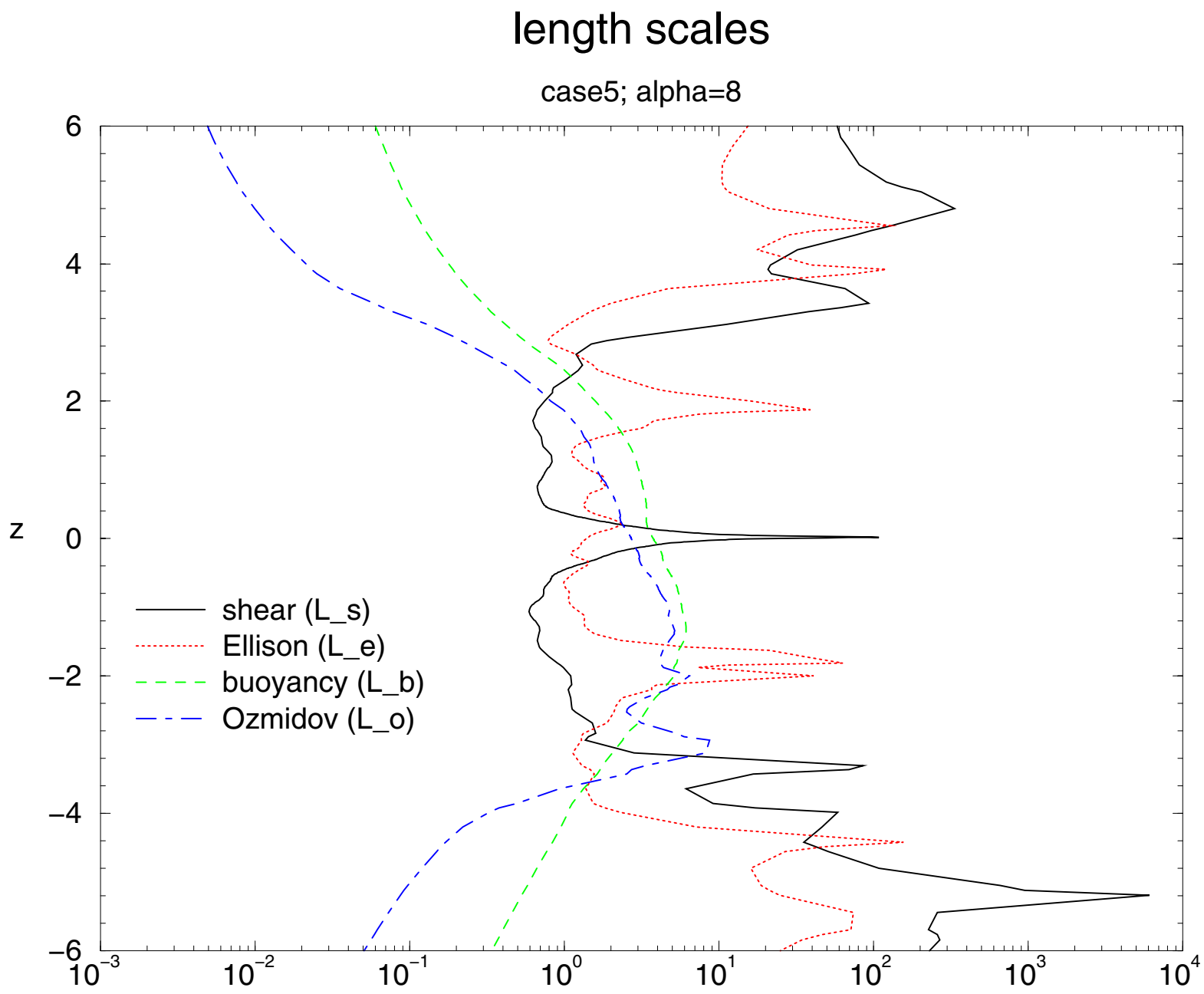
length scales
case5; alpha=8
z
6
4
2
0
−2
−4
−6
10^{-3}
10^{-2}
10^{-1}
10^{0}
10^{1}
10^{2}
10^{3}
10^{4}
shear (L_s)
Ellison (L_e)
buoyancy (L_b)
Ozmidov (L_o)

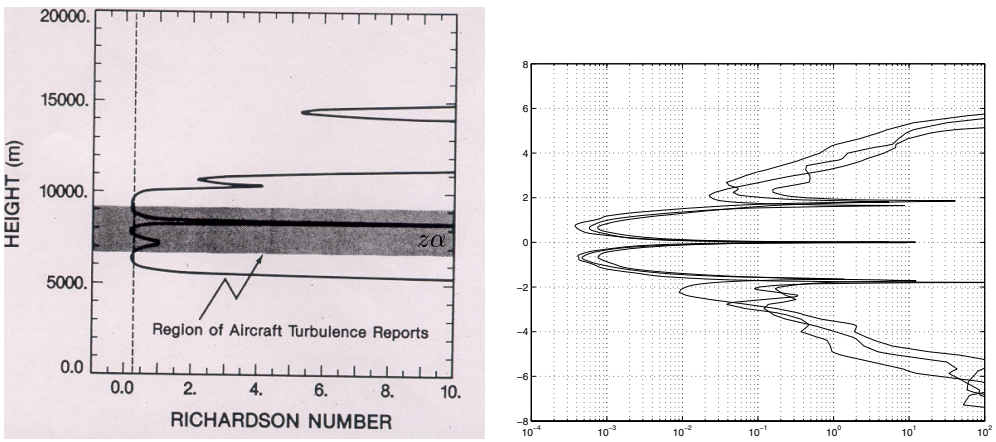

(a) (b)

Figure 1: (a) An example of a gradient Richardson number profile corresponding to Fig. 1(a), measured by Bedard et al. (1986)(reproduced with permission from the American Meteorological Society); (b) Gradient Richardson number profiles at quasi-equilibrium from the numerical simulations for Case 5, 6 ($256^2 \times 512$ resolution) and Case 7 ($512^2 \times 1024$ resolution).

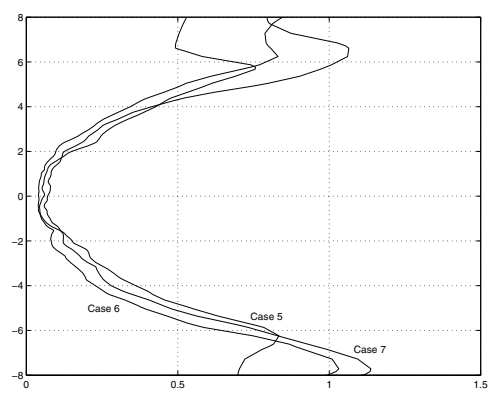

Ratios of Turbulence Outer Scales are independent of Reynolds numbers.

Conclusions and Impact on ABL/ADA (Atmospheric Decision Aid)

- Mesoscale-microscale coupling (nested approach, outer grid from WRF/MM5 profiles).
- Initialization of unbalanced dynamics (thermal wind unbalance, geostrophic departure, divergent velocity potential).
- Non-Gaussianity (PDF and skewness strongly z-dependent).
- Anisotropic, non-Kolmogorov turbulence: diagnostic via collapse of outer length scales.
- Two layers of strong refractive turbulence on sides of jet stream.

- Mechanical turbulence vs. optical turbulence: peaks of velocity variances and temperature variance (C_n^2) are in different vertical locations (velocity variance peak much closer to core of jet).
- Evidence separation between layers of enhanced optical turbulence and peaks of mechanical turbulence (they are coupled but well separated).
- The above separation depends on the mesoscale structure of the jet.
- Variability and statistics of turbulence outer scales.
- Shear and Tatarskii scales should be used for parameterization of enhanced layers of C_n^2, not the buoyancy (Deardorff) outer scale.